Liu, J., **Wu, L.**, **Kümmel, S.**, Yao, J., Schaefer, T., Herrmann, H., **Richnow, H.-H.** (2018):
Carbon and hydrogen stable isotope analysis for characterizing the chemical degradation of tributyl phosphate
Chemosphere **212** , 133 – 142

http://dx.doi.org/10.1016/j.chemosphere.2018.08.034

Carbon and hydrogen stable isotope analysis for characterizing the chemical degradation of tributyl phosphate

Jia Liu[1,2 §], Langping Wu[2 §], Steffen Kümmel[2], Jun Yao[3], Thomas Schaefer[4], Hartmut Herrmann[4], Hans-Hermann Richnow[2,3*]

[1]School of Energy and Environmental Engineering, University of Science and Technology Beijing, Xueyuan Road No.30, Haidian District, Beijing 100083, PR China

[2]Department of Isotope Biogeochemistry, Helmholtz Centre for Environmental Research-UFZ, Permoserstraße15, Leipzig 04318, Germany

[3]School of Water Resources and Environment, China University of Geosciences (Beijing), Xueyuan Road No.29, Haidian District, Beijing 100083, PR China

[4]Atmospheric Chemistry Department (ACD), Leibniz Institute for Tropospheric Research (TROPOS), Permoserstraße15, Leipzig 04318, Germany

§ Dual-first authorship: the two authors have contributed equally to this work.

* To whom correspondence should be addressed:

E-mail: hans.richnow@ufz.de Tel.: +49 (0) 341 235 1212, Fax: +49 (0) 341 2351443

Abstract

Tributyl phosphate (TBP) belongs to the group of trialkyl substituted organophosphate esters. Its chemical reactivity depends on the stability of various chemical bonds. TBP was used as a model compound for the development of a concept using stable isotope fractionation associated with bond cleavage reactions for better understanding the fate of TBP in the environment. Carbon isotope enrichment factors (ε_C) of TBP hydrolysis were found to be pH dependent (-3.8 ± 0.3‰ at pH 2, -4.6 ± 0.5‰ at pH 7, -2.8 ± 0.1‰ at pH 9, no isotope fractionation at pH 12), which is in accordance with the mode of a S_N2 hydrolytic bond cleavage. Hydrogen isotope fractionation was negligible as no H bond cleavage is involved during hydrolysis. The apparent carbon kinetic isotope effect ($AKIE_C$) ranged from 1.045 to 1.058. In contrast to hydrolysis, both carbon and hydrogen isotope fractionation were observed during radical oxidation of TBP by $^{\bullet}OH$ and $SO_4^{\bullet-}$, yielding ε_C from -0.9 ± 0.1‰ to -0.5 ± 0.1‰ and ε_H from -20 ± 2‰ to -11 ± 1‰. $AKIE_C$ and $AKIE_H$ varied from 1.007 to 1.011 and from 1.594 to 2.174, respectively. The correlation of ^2H and ^{13}C fractionation revealed Λ values ranging from 17 ± 1 to 25 ± 6. Results demonstrated that the correlation of ^2H and ^{13}C isotope fractionation of TBP allowed to identify radical reactions and to distinguish them from hydrolysis. The presented dual isotope analysis approach has diagnostic value for characterizing the chemical transformation of TBP in the environment.

Keywords

Tributyl phosphate, isotope fractionation, hydrolysis, radical oxidation, AKIE

1. Introduction

Tributyl phosphate (TBP) is an organophosphorus compound widely used as flame retardant, plasticiser, anti-foamer, component of herbicides and hydraulic fluids (Regnery et al., 2011). In addition, it was extensively used as a solvent for plutonium uranium redox extraction (PUREX) for nuclear fuel reprocessing (Mincher et al., 2008). The production of commercially used TBP is about 3000-5000 tons/year in Europe (Nancharaiah et al., 2015). Due to its extensive use, TBP is frequently detected in the aquatic environment of many countries, including Germany (Fries and Püttmann, 2003; Regnery and Puttmann, 2010), Austria (Martinez-Carballo et al., 2007), Italy (Bacaloni et al., 2008), Spain (Rodil et al., 2012), Korea (Lee et al., 2016), and China (He et al., 2014; Shi et al., 2016).

TBP can inhibit the enzyme acetylcholine esterase (AChE), resulting in cholinergic toxicity of the autonomic system and can thus lead to respiratory paralysis and even death (Bergman et al., 2012; Greget et al., 2016). Given these adverse effects, TBP has been an environmental concern for decades, especially in aquatic systems. The main degradation pathways are hydrolysis, indirect photo-oxidation or microbial degradation (Berne et al., 2005; Watts and Linden, 2009; Nancharaiah et al., 2015; Su et al., 2016). These are probably the key processes how TBP is degraded or attenuated in the environment. Direct chemical oxidation is effective for the removal of organic contaminants in waste water. In particular, chemicals, such as hydrogen peroxide, persulfate, permanganate and ozone, have been applied for in situ chemical oxidation (ISCO) for the treatment of subsurface TBP or similar contamination (Watts and Teel, 2006). Hydroxyl radicals ($^{\bullet}$OH) are an effective oxidant with redox potential of 1.7–2.8 V and are frequently used for wastewater remediation (Waclawek et al., 2017). Similar to $^{\bullet}OH$, the sulfate radical ($SO_4^{\bullet-}$) with a redox potential of 2.5–3.1 V is efficient for the oxidation of many organic compounds (Neta et al., 1988). $SO_4^{\bullet-}$ can be generated for example from peroxydisulfate ($S_2O_8^{2-}$, PS) or peroxymonosulfate ($HS_2O_5^{-}$) salts by the activation of the persulfate anion ($S_2O_8^{2-}$, $E_0 = 2.01$ V) using light (Herrmann, 2007; Yang et al., 2017) or heat (House, 1962; Liang and Su, 2009). Over the past ten years, considerable attention has been paid to potassium peroxydisulfate (KPS) because of its lower cost compared to H_2O_2 or O_3 and the high efficiency for organic mineralization (Lau et al., 2007; Waclawek et al., 2017).

Conventionally, degradation pathways are chemically analysed by measuring the concentrations decrease of reactants and the appearance of degradation products for the identification of reaction products. However, this approach often has large uncertainties because of the influence of physical processes (such as dilution, volatility and sorption), the challenges of detecting unknown products and the difficulties to establish mass balances. As an alternative technology, compound specific isotope analysis (CSIA) making use of isotope fractionation processes of degradation reactions can be used for the qualitative characterisation and quantitative estimation of processes involved in organic compound degradation in the environment. This technique is becoming a routine and practical approach in biogeochemistry and environmental science (Elsner, 2010; Thullner et al., 2012; Nijenhuis and Richnow, 2016; Vogt et al., 2016).

For better understanding of the transformation mechanisms, the kinetic isotope effect (KIE) based on chemical bond change reactions can be analyzed. The KIE characterizes the rate limitation of a bond change reaction posed by isotopologues. The rate limitation is equivalent to the stability of heavy and light isotope substituted bonds and characterizes the transition state of a chemical reaction (Northrop, 1981; Wolfsberg et al., 2009). The apparent kinetic isotope effect (AKIE) can be calculated to normalize the isotope enrichment factor (ε) for non-reacting positions and intermolecular competition to compensate for "dilution" of the isotope composition in reacting isotopologues. The AKIE can be used to compare the kinetic isotope effect of bond cleavage reactions of different molecules. Multi-element isotope fractionation analysis correlating the isotope fractionation of two (or more) elements can be used to evaluate the degradation pathways (Gray et al., 2002; Elsner et al., 2005). Previous studies demonstrated the potential use of stable isotope fractionation for characterizing the transformation mechanisms of organophosphorus compounds, such as dichlorvos, dimethoate, methyl parathion, parathion and tris(2-chloroethyl) phosphate (Wu et al., 2014; Wu et al., 2017; Wu et al., 2018a).

In the present study, we systematically examined the carbon and hydrogen isotope fractionation upon hydrolysis of TBP under acidic, neutral and alkaline conditions to characterize the reaction pathways. The isotope fractionation patterns of TBP by radical oxidation ($SO_4^{\bullet-}$ and $^{\bullet}OH$) were also examined. The objectives of this study were to (1) investigate the kinetic reaction rate constant k_{obs} of hydrolysis and radical oxidation; (2) characterize the stable carbon and hydrogen isotope fractionation of TBP during hydrolysis and radical oxidation; (3) distinguish different mechanisms by using the AKIE values and correlating ^{2}H and ^{13}C isotope fractionation to obtain Λ values, which may be used diagnostically for tracing TBP degradation in the field.

2. Materials and methods

A detailed description of the analytical methods is provided in the Supplementary Information (SI).

2.1 Chemicals

All chemicals were of analytical grade quality and used without further purification. Tributyl phosphate (TBP, 99% purity) and dibutyl phthalate (DBP, >99% purity) were purchased from Xiya Company (China). Dichloromethane (DCM) was supplied by Carl Roth GmbH + Co. KG (Karlsruhe, Germany). Potassium peroxydisulfate ($K_2S_2O_8$), hydrogen peroxide (30% H_2O_2), di-potassium hydrogen phosphate (K_2HPO_4), potassium dihydrogen phosphate (KH_2PO_4), sodium hydrogen carbonate ($NaHCO_3$), sodium hydrate (NaOH), and disodium hydrogen phosphate (Na_2HPO_4) were supplied by Merck (Guaranteed reagent quality, Darmstadt, Germany). Solutions and pH buffers were prepared in ultrapure water obtained by a Milli-Q System (Millipore GmbH, Germany).

2.2 Hydrolysis and radical oxidation experiments

The following buffer solutions were used to obtain hydrolysis at different pH conditions: KCl-HCl (50 mM for pH 2), K_2HPO_4-KH_2PO_4 (100 mM for pH 7), $NaHCO_3$-NaOH (45.5 mM for pH 9), and Na_2HPO_4- NaOH (32.5 mM for pH 12).

Hydrolysis experiments: TBP is hydrolyzed with very slow reaction rates at room temperature under neutral to acidic conditions but rapidly hydrolyzed under strong alkaline condition (Su et al., 2016). In order to adjust the hydrolysis rates in the same order of magnitude for a better comparison of the isotope fractionation patterns associated with different reaction pathways, hydrolysis experiments were carried out at 80 °C to accelerate the hydrolysis rate at pH 2, pH 7 and pH 9, respectively. Hydrolysis experiments at pH 12 were performed at 35 °C to slow down the reaction. All experiments were conducted in 40 mL buffer solutions in 150-mL serum bottles with 100 mg L^{-1} TBP as initial concentration. At different time intervals, the reaction solutions were extracted by adding 1 mL DCM containing 1000 mg L^{-1} DBP as internal standard and shaking for at least 4 h at 10 °C. Extracts were stored at 4 °C prior to analysis. The extraction recovery and effect of the extraction procedure on carbon and hydrogen isotope signature were evaluated as described in Section 3 of the Supplementary Information.

Potassium peroxydisulfate (KPS) oxidation: For KPS oxidation experiments a molar ratio of TBP to KPS of 1:20 was used. The KPS oxidation reaction was not conducted at pH 2 due to the exclusive formation of secondary radicals and complicating subsequent reactions. At pH 2, the $SO_4^{\bullet-}$ reacts exclusively with the Cl^- from the HCl/ KCl buffer to produce a Cl atom, which will subsequently react to form $Cl_2^{\bullet-}$, a dichloride radical anion (Herrmann, 2003). Therefore, the KPS oxidation reactions were only conducted at pH 7, pH 9 and pH 12, respectively. The initial concentration of TBP was 100 ppm. Buffer solutions with different pH values were prepared as described above. All KPS oxidation reactions were carried out at 35 °C. Control experiments were carried out without the addition of KPS. Remaining TBP was extracted and analyzed as described in the hydrolysis experiment.

UV/H_2O_2 oxidation experiment: Photolysis experiments were carried out at pH 7 in phosphate buffer with 200 mg L^{-1} initial TBP concentration. Irradiation was achieved by

150 W xenon lamp (Type no. L2175, Hamamatsu, Japan), which covered a broad continuous spectrum from 185 nm to 2000 nm. A long-pass filter with a cut-off of short UV wavelengths below 280 nm (20CGA-280, Newport Corporation, Irvine, U.S.) was applied. Direct photolysis is not expected at the applied UV wavelengths due to the almost negligible photon absorption by TBP (Watts and Linden, 2009). The molar ratio of TBP to H_2O_2 was 1:5. In order to investigate the effects of buffer solution concentrations and reaction rates on the isotope fractionation of TBP, three experiments were carried out in 100 mM buffer solution at 20 °C (UV/H_2O_2_1), 100 mM buffer solution at 15 °C (UV/H_2O_2_2) and 10 mM buffer solution at 15 °C (UV/H_2O_2_3), respectively. 100 mM buffer solution was applied to make sure that the pH will remain stable at 7 during the reaction. Lower buffer concentration of 10 mM was applied to minimize the formation of the secondary radicals (SI, section 5). The experiments were conducted at different temperature of 20 °C and 15 °C to slow down the reaction rate. For direct photolysis, experiments were conducted under the same conditions but without the addition of H_2O_2 in a 100 mM buffer solution at 20 °C. Dark control experiments were conducted under identical experimental conditions without UV exposure (100 mM buffer solution). More information on the experimental setup of the UV degradation experiments are described elsewhere (Zhang et al., 2016). The transformation products of TBP in UV/H_2O_2 experiments were tentatively analyzed by a Fourier-transform ion cyclotron resonance mass spectrometer (FT-ICR MS, Solarix XR 12T, Bruker Daltonics), the analytical procedures were described in SI.

2.3 Data analysis

Isotope ratios were expressed as delta notation (δ^{h}E) in parts per thousand (‰) based on Eq. [1]. Here, R_{sample} is the ratio of the heavy (^{h}E) to the light isotopes (^{l}E) of a sample and R_{ref} corresponds to the ratio of the respective isotopes of reference. For stable carbon isotope analyses the Vienna Pee Dee Belemnite (V-PDB) is used as reference, whereas for stable hydrogen isotope analyses the Vienna Standard Mean Ocean Water (V-SMOW) is applied (Coplen, 1996).

$$\delta\, ^{h}\mathrm{E} = \left(\frac{\mathrm{R}_{sample}}{\mathrm{R}_{ref}} - 1\right) = \left(\frac{^{h}\mathrm{E}/\ ^{l}\mathrm{E}}{^{h}\mathrm{E}_{ref}/\ ^{l}\mathrm{E}_{ref}} - 1\right) \qquad [1]$$

The isotope enrichment factor (ε_E) can be determined from the logarithmic form of the Rayleigh equation, as shown in Eq. [2] (Rayleigh, 1896; Elsner, 2010). The variables $\delta^{h}E_t$ and $\delta^{h}E_0$ are the isotope compositions of a compound for the element E at time t and time zero, respectively, and f is the residual substrate fraction. The changes in concentration during the reaction (C_t/C_0) can be related to the changes in isotope composition by ε_E.

$$\ln\left(\frac{\delta^{h}\mathrm{E}_t+1}{\delta^{h}\mathrm{E}_0+1}\right) = \varepsilon_E \cdot \ln f = \varepsilon_E \cdot \ln\left(\frac{\mathrm{C}_t}{\mathrm{C}_0}\right) \qquad [2]$$

The AKIE_E value of the bond cleavage at the reactive position can be calculated with Eq. [3], where n is the total number of atoms for element E in the molecule, x is the number of reactive sites, and z is the number of indistinguishable reactive sites (Elsner et al., 2005). The normalisation of AKIE_E corrects the bulk isotope enrichment for non-reactive positions and the intramolecular isotopic competition.

$$\mathrm{AKIE} = \frac{1}{1 + \frac{n}{x} \times \mathrm{z} \times \varepsilon} \qquad [3]$$

Assuming that two processes (process 1 and 2) are reacting with the same substrate simultaneously and both processes follow first-order kinetics, the contribution of the individual processes in the mixed reaction can be estimated by an extended Rayleigh-type equation using the individual isotope enrichment factors of the particular reaction (ε_1 and ε_2). The observable ε_i of the mixed reaction and the ε_1 and ε_2 of the individual pathway 1 and 2 are needed for this calculation. The rate ratio of two competing degradation pathways (F) can be calculated by Eq. (4) (Van Breukelen, 2007), indicating the isotope fractionation contributed by pathway 1 to the observed ε_i.

$$F = \frac{\varepsilon_i - \varepsilon_2}{\varepsilon_1 - \varepsilon_2} \qquad [4]$$

3. Results

3.1 *Effects of extraction on isotope signature*

The recovery of the liquid/liquid DCM extraction method was 91.2 ± 10.2% (Fig. S2 (a)). The isotope shifts of TBP before and after DCM extraction were 0.05 – 0.65‰ for $\delta^{13}C$, and 1 – 4‰ for $\delta^{2}H$ (Fig. S2 (b)), respectively. Considering the analytical uncertainty of carbon and hydrogen isotope compositions, which is < ±0.5‰ and < ±5‰ for carbon and hydrogen, respectively, carbon and hydrogen isotope shifts due to the extraction process are insignificant. A detailed description was provided in SI, section 3.

3.2 *Isotope fractionation of TBP during hydrolysis*

The degradation curves and changes in carbon and hydrogen isotope compositions of TBP are illustrated in Fig. 1, and the obtained k_{obs} and ε values for TBP hydrolysis are summarized in Table 1. All hydrolysis experiments followed pseudo-first order kinetics with R^2 better than 0.97, alkaline conditions resulted in higher reaction rates compared to neutral and acidic conditions (pH 12 > pH 9 > pH 7 ≈ pH 2) (Table 1). The stable carbon isotope enrichment could be quantified by the Rayleigh equation. At pH 2, 90% degradation was achieved within 1236 h, resulting in a carbon enrichment factor (ε_C) of -3.8 ± 0.3‰. 88% degradation was achieved within 1140 h at pH 7, yielding an ε_C of -4.6 ± 0.5‰. 94% degradation was achieved within 864 h and yielding an ε_C of -2.8 ± 0.1‰ at pH 9. At pH 12, 80% degradation was achieved after 1464 h and no carbon enrichment was observed. Hydrogen isotope fractionation was not observed in all hydrolysis experiments (Fig. 1).

3.3 Isotope fractionation of TBP during KPS oxidation

The degradation curves and changes in carbon and hydrogen isotope compositions of TBP are illustrated in Fig. 2, and the corresponding k_{obs} and ε values are summarized in Table 1. All oxidation experiments followed pseudo-first order kinetics and the k_{obs} values decreased with increasing pH (Table 1). The stable carbon and hydrogen isotope fractionation could be quantified by the Rayleigh equation. About 95% TBP was degraded within 292 h at pH7/KPS, resulting in a ε_C = -0.9 ± 0.1‰ and ε_H = -16 ± 2‰, respectively. At pH9/KPS, 95% degradation was achieved within 332 h, yielding an ε_C of -0.8 ± 0.1‰ and an ε_H of -20 ± 2‰. At pH12/KPS, TBP was depleted to 90% within 400 h, corresponding to an ε_C = -0.5 ± 0.1‰ and ε_H = -11 ± 1‰. No degradation took place in control experiments except for pH12/KPS (Fig. S2). Due to the hydrolysis at pH 12, 35% of TBP was degraded within 400 h.

3.4 Isotope fractionation of TBP during UV/H_2O_2 oxidation

Degradation curves and changes in carbon and hydrogen isotope compositions of TBP are illustrated in Fig. 2. All experiments followed pseudo-first order kinetics, and the k_{obs} values (× 10^{-3} h^{-1}) were 474.2 ± 11.4 in UV/H_2O_2_1, 27.9 ± 2.4 in UV/H_2O_2_2 and 6.8 ±

0.5 in UV/H_2O_2_3, respectively (Table 1). All coefficients of determination (R^2) were larger than 0.99. In the experiment UV/H_2O_2_1, 96% TBP was degraded within 6.7 h, yielding a ε_C of -0.8 ± 0.1‰ and ε_H of -14 ± 1‰. In the degradation experiment UV/H_2O_2_2, 85% TBP was depleted in 72.5 h, resulting in a ε_C of -0.6 ± 0.3‰ and ε_H of -13 ± 3‰. In the degradation experiment UV/H_2O_2_3, 93% TBP was transformed within 385 h, and an ε_C of -0.6 ± 0.2‰ and ε_H of -17 ± 7‰ were obtained. In the control experiment without H_2O_2 employing the conditions used in UV/H_2O_2_1, no significant change of the TBP concentration was observed (Fig.S2 d), suggesting that direct photolysis did not take place during these experiments.

3.5 Analysis of transformation products of TBP in the UV/H_2O_2 experiment

Three potential transformation products were tentatively characterized as di-n-butylphosphate (P1), keto-tri-butylphosphate (P2), and hydroxy-tri-butylphosphate (P3) (Table S1 and Fig. S3). The detailed information of characterized transformation products is given in the SI, section 7. The precise position of the hydroxyl or keto group at the side chain of the TBP molecule could not be confirmed, however, it is likely that the functional group is formed by radical attack at the sub-terminal carbon of the butyl chain.

3.6 Two dimensional isotope fractionation (C-H)

In order to explore the diagnostic potential of two dimensional isotope fractionation analysis, the hydrogen and carbon isotope fractionation were plotted to obtain Λ values ($\Lambda = \frac{\Delta^2H}{\Delta^{13}C} \approx \frac{\varepsilon_H}{\varepsilon_C}$, $\Delta^{13}C = \delta_t{}^{13}C\text{-}\delta_0{}^{13}C$, $\Delta^2H = \delta_t{}^2H\text{-}\delta_0{}^2H$). However, due to the absence of hydrogen isotope fractionation Λ could not be defined for hydrolysis. In contrast, the radical oxidation of TBP under pH7/KPS, pH9/KPS and pH12/KPS conditions resulted in Λ values of 17 ± 1, 23 ± 1, 19 ± 1, respectively (Table 1). The reactions of TBP by

UV/H_2O_2 (dominant $^{\bullet}OH$ reaction, described in SI, section 5) yielded an average Λ value of 20 ± 4 (Table 1), which is statistically identical with the ones obtained from KPS oxidation experiments. The two dimensional isotope fractionation analysis of all radical oxidation experiments including $SO_4^{\bullet-}$ and $^{\bullet}OH$ gave an average Λ value of 20 ± 4 (Table 1).

4. Discussion

4.1 Insight of the isotope fractionation during hydrolysis

A previous study proposed two hydrolysis pathways of organophosphorus compounds (OPs) (Fig. 3a,b): the first one is OH^- or H_2O attacks the phosphorus atom; the second one is H_2O attacks the carbon atom (Wu et al., 2006). The acid-catalysed hydrolysis of esters mainly proceeds via an $A_{AC}2$ mechanism suggesting an acyl-oxygen fission (AC) in a bimolecular reaction (Day and Ingold, 1941). For instance, under acidic and neutral conditions, trimethyl phosphate may lead to a C–O bond split as demonstrated in experiments with ^{18}O-labelled water as indicator (Blumenthal and Herbert, 1945). Consequently, the C-O bond cleavage leads to carbon isotope fractionation of TBP. At high pH (e.g., pH >10), OH^- attacks the phosphorus atom through simple nucleophile displacement (S_N2-type) leading to a P–O bond cleavage (Wanamaker et al., 2013). The reaction may proceed via a two-step addition-elimination pathway involving a pentacoordinate intermediate, such as TS1 and TS2 (Fig. 3b) (Kirby et al., 2013). The observed negligible carbon and hydrogen isotope fractionation of TBP at pH 12 highly supports a P–O bond split.

At pH 9, the observed carbon isotope fractionation of TBP provided evidence for a C–O bond split. However, the ε_C value at pH 9 was lower than that of pH 2 and pH 7. The same phenomenon was observed during methyl parathion and ethyl parathion hydrolysis (Wu et al., 2018a). Given that hydrolysis of OPs is pH dependent, no precise pH boundary can be used for the identification of C–O or P–O bond split. The two major degradation pathways occurred simultaneously at pH 9. The P–O bond cleavage is not associated with carbon isotope fractionation, and thus carbon isotope fractionation can be solely attributed to the splitting of the C–O bond. Considering that the carbon fractionation observed in experiments for acid hydrolysis (pH 2) and alkaline hydrolysis (pH 12) are representative for the mechanism for C–O and P–O bond split respectively, and both processes follow the first-order kinetics, Eq. [4] can be applied for the calculation of the contribution of the two pathways acting during the hydrolysis at pH 9. The carbon isotope enrichment factors of hydrolysis at pH 2 (ε_1 = -3.8 ± 0.3‰) and the ε_2 value of 0‰ representing hydrolysis at pH 12 were used for calculation. Within the uncertainty of isotope enrichment factors observed in the experiments, the enrichment factor of TBP at pH 9 (ε_i = -2.8±0.1‰) suggests that 67–80% of TBP was hydrolysed via the C–O bond cleavage pathway, and the remaining 20–33% was attributed to the P–O bond split. The mechanism of acidic and neutral hydrolysis is almost identical, and the calculation is also valid for comparing contributions at neutral conditions.

For testing the hypothesis of the degradation mechanisms the AKIE values were compared to intrinsic KIE reactions. For TBP hydrolysis, AKIE$_C$ (calculation is described in SI, section 6) ranged from 1.048 to 1.058, which is in line with the intrinsic KIE values of nucleophilic substitution (1.03–1.09; S$_N$2 type on C–O bond) (Paneth et al., 1992), supporting the conclusion of C–O bond cleavage during TBP hydrolysis.

4.2 pH-dependency of radical oxidation

In this study, either $SO_4^{\bullet-}$ or $^{\bullet}OH$ was involved in persulfate oxidation, which is a pH-dependent reaction. Once $SO_4^{\bullet-}$ was generated by $S_2O_8^{2-}$ scission, it could propagate a chain of reactions involving the formation of other reactive species. $SO_4^{\bullet-}$ can react with water at all pH levels, forming $^{\bullet}OH$ (Eq. [S1]) (Neta et al., 1988; Herrmann et al., 1995). With the increase of pH, $SO_4^{\bullet-}$ preferentially reacts with OH^- forming $^{\bullet}OH$ with an increasing rate constant (Eq. [S2]) (Neta et al., 1988; Herrmann et al., 1995). Hence, at low pH (i.e. pH 7), $SO_4^{\bullet-}$ is the predominant reactive species, whereas at pH 9, both $SO_4^{\bullet-}$ and $^{\bullet}OH$ could coexist and at pH 12, $^{\bullet}OH$ is predominant (Liang and Su, 2009). Considering both radical species can be quenched to some extent by the PO_4^{3-} and CO_3^{2-} components in the buffer, the contributions of secondary radicals formed during the reaction and subsequent reaction with TBP were taken into account and the contributions were estimated to be minor (description in SI, section 5).

During radical oxidation of TBP, the rate constants have the following order: pH 7 > pH 9 > pH 12 (Table 1), demonstrating that the reaction can be retarded by increasing pH. The rate constants are associated with the reactivity of the radicals as $SO_4^{\bullet-}$ has a stronger redox potential than $^{\bullet}OH$ (Buxton et al., 1988; Neta et al., 1988), and thus may result in larger kinetic rate constants. The TBP oxidation by KPS at pH 12 had a 5 times larger rate constant compared to the hydrolysis at pH 12 (Table 1) suggesting that radical oxidation was dominating the degradation reaction. Nevertheless, two degradation processes co-existed in the degradation of TBP in the pH12/KPS system, namely, radical oxidation and alkaline hydrolysis. The contribution of alkaline hydrolysis on the TBP degradation was 35% based on the control experiment without the addition of KPS (Fig. S2).

4.3 Insight of isotope fractionation during $^{\bullet}OH$ and $SO_4^{\bullet-}$ reaction with TBP

$^{\bullet}OH$ which can be generated by H_2O_2 under UV irradiation has a high tendency to react non-selectively on functional groups via electron transfer, hydrogen abstraction or electrophilic/radical addition (Buxton et al., 1988). The transformation products formed in the UV/H_2O_2 reaction with TBP were tentatively identified as keto and hydroxylated derivatives (Table S1), suggesting a hydrogen abstraction from the alkyl chain at sub-terminal positions. This suggests a formation of a radical at the side chain which is quenched by oxygen forming a meta stable intermediate radical followed by a Russell mechanism (Russell, 1957) to form keto and hydroxyl TBP (Fig. 3c). In subsequent steps further reactions may lead to the formation of dibutyl phosphate. The hydrogen abstraction mechanism will lead to ^2H and ^{13}C isotope fractionation of TBP. Alternatively, radical addition, for example $^{\bullet}OH$ addition to the central phosphorus atom, may form a $(C_4H_9O)_3PO^{\bullet}OH$ radical leading to elimination of butanol and resulting in dibutyl phosphate (Fig. 3c). However, $^{\bullet}OH$ addition to phosphate will lead to P-O cleavage and is unlikely to induce ^2H and ^{13}C isotope fractionation. Similar mechanisms have been observed in previous studies during the $^{\bullet}OH$ reaction with tri-(2chloroethyl) phosphate (Wu et al., 2018a) and dimethyl phenylphosphonate (Oh et al., 2003). According to the reaction mechanisms of $SO_4^{\bullet-}$ and tri-(2chloroethyl) phosphate, $SO_4^{\bullet-}$ was reported to react with phosphorus and carbon atoms, thereby causing a P–O and C–H bond split (Ou et al., 2017). Similarly, two pathways were proposed to be involved in TBP oxidation induced by $SO_4^{\bullet-}$. One pathway involves the addition to the phosphorus centre and rupturing of $–OCH_2CH_2CH_2CH_3$ chains and the other one involves the addition to the $–CH_2–$ moieties causing the C–H bond split.

The radical reaction with the alkane side chain at the sub-terminal position cleaving a C-H bond in the transition state leads to ^2H and ^{13}C isotope fractionation. The observed ^2H and ^{13}C isotope fractionation in our experiments showed that this pathway took place during radical oxidation of TBP by $^{\bullet}OH$ and $SO_4^{\bullet-}$. The obtained ε_C and ε_H at pH7/KPS ($SO_4^{\bullet-}$ dominating) and pH9/KPS ($SO_4^{\bullet-}$ and $^{\bullet}OH$ co-existing) were very similar with the ones from UV/H_2O_2 (pure $^{\bullet}OH$) (Table 1). The slightly smaller ε_C of -0.5±0.1‰ and ε_H of -11±1‰

at pH12/KPS ($^{\bullet}OH$ dominating) is due to the effect of alkaline hydrolysis of TBP at pH 12. Considering 35% of TBP degradation was contributed by alkaline hydrolysis (process 1) at pH12/KPS (Fig. S2), the ε associated with the $^{\bullet}OH$ oxidation process (process 2) can be estimated using Eq. (4) where F = 0.35, ε_i = -0.5±0.1‰ for carbon and -11±1‰ for hydrogen, ε_1 = 0‰. Thus, ε_2 was calculated to be -0.8±0.2‰ for carbon and -17±2‰ for hydrogen, which were identical with the ones obtained from radical oxidation of TBP at pH7/KPS, pH9/KPS and UV/H_2O_2 conditions (Table 1). The average values of ε_C = -0.7±0.1‰, ε_H = -16±3‰, and Λ = 20±4 calculated from all individual radical oxidation experiments suggest that $SO_4^{\bullet-}$ and $^{\bullet}OH$ radical oxidation processes of TBP could not be distinguished based on isotope enrichment factors within the uncertainty of our results, and it may suggest that both reaction processes had similar mechanisms of attacking carbon atoms and cleaving C–H bonds. However, P–O bond splitting cannot be characterized by the ^2H and ^{13}C isotope fractionation of TBP in this study, therefore, ^2H and ^{13}C isotope fractionation studies cannot provide direct evidence to evaluate the process of P–O bond cleavage.

The $AKIE_C$ which ranged from 1.007 to 1.011 for all radical oxidation experiments (Table 1) is consistent with those reported for *n*-alkanes' chemical transformation (1.01–1.02) (Bouchard et al., 2008) and lower than the Streitwieser Limits for a C–H bond (1.021) cleavage (Elsner et al., 2005). A series of studies yield $AKIE_H$ values between 2–23 that are typical for H-bond cleavage (Elsner et al., 2005). The $AKIE_H$ values reported in this study were lower and ranged from 1.608 to 2.174, indicating that steps other than the C–H bond cleavage were also rate-determining for radical oxidation of TBP. Potentially a radical reaction at the phosphate moiety may contribute to TBP degradation (Fig.3c 2) but do not contribute to ^2H and ^{13}C isotope fractionation. This may explain why the calculated AKIE values are lower than those typically expected for C-H bond cleavage. In our case the calculated AKIE values do not describe the KIE of the C-H bond cleavage at the side chain of TBP because the overall transformation reaction has a contribution of OH addition to the phosphate. However our current data do not allow validating this hypothesis in more detail.

4.4 Identification of degradation pathways by 2D-plot to analyse Λ values

The $SO_4^{•-}$ and $^{•}OH$ resulted in a characteristic isotope fractionation pattern (Λ values) for radical oxidation reactions of TBP. As hydrolysis did not lead to primary hydrogen isotope effects, hydrolysis and radical oxidation of TBP can be clearly distinguished by the correlation of ^{2}H and ^{13}C fractionation (Fig. 4). Similar results have been reported for radical oxidation of tris(2-chloroethyl) phosphate by $^{•}OH$ formed in Fenton reactions and UV/H_2O_2 (Wu et al., 2018a). However, considering the obtained identical Λ values (section 3.5), the Λ values do not allow for separating the mechanisms of $SO_4^{•-}$ and $^{•}OH$ reactions with TBP. The Λ values are not affected when non-isotope-fractionating processes such as alkaline hydrolysis are influencing overall degradation, showing that mechanisms can also be identified when non-isotope-fractionating processes are at work. This may imply that the extent of isotope fractionation can be used for the assessment of radical reactions and may allow for the selection of an isotope enrichment factor representative for radical reactions. This isotope enrichment factor could then be used to calculate the contribution of degradation of TBP by radical reactions to the overall degradation in the environment. For example the hydrogen enrichment factor could be used to quantify the contribution of radical reactions because hydrolysis does not exhibit ^{2}H fractionation. The ^{2}H and ^{13}C isotope fractionation pattern of parathion has been used at an industrial dumpsite to characterise the contribution of neutral and acidic hydrolysis of parathion in a remediation measure (Wu et al., 2018b). Similarly, the Λ values determined throughout the current study could be used in the future to characterise degradation reaction in field studies for quantifying hydrolysis or chemical oxidation reactions. Further information for quantification of degradation reactions in the environment using enrichment factors have been summarised previously (Thullner et al., 2012).

5. Conclusions

In this study, the carbon and hydrogen isotope fractionation caused by hydrolysis and radical oxidation of TBP were systematically examined at different pH conditions. The $AKIE_C$ of the hydrolysis under neutral and acidic conditions was 1.048 - 1.058, which was consistent with an S_N2-type displacement reaction cleaving the C-O bond. At pH 12, a S_N2-type nucleophilic displacement reaction cleaving the P-O bond was characterized by the absence of carbon and hydrogen isotope fractionation. During hydrolysis at pH 9, the S_N2-type displacement reaction cleaving the C-O bond affects the carbon isotope fractionation and contributes to 67 - 80% of the overall reaction. The radical oxidation of TBP results in $AKIE_C$ and $AKIE_H$ of 1.007 – 1.011 and 1.608 - 2.174, respectively, which is consistent with a major contribution of a C-H bond cleavage. The correlation of ^2H and ^{13}C isotope fractionation of TBP allows identifying radical reactions and distinguishing radical reactions from hydrolysis.

Acknowledgements

Jia Liu and Langping Wu were financially supported by the China Scholarship Council (File No. 201506460057 and 201306460007, respectively). The work was partially supported by the National Science Foundation of China [grant number 41430106, 2014 and 41573080, 2015]. The authors are grateful for using the analytical facilities of the Centre for Chemical Microscopy (ProVIS) at the Helmholtz Centre for Environmental Research – UFZ, which is supported by the European Regional Development Funds (EFRE - Europe funds Saxony) and the Helmholtz Association. The authors thank Dr. Oliver J. Lechtenfeld for his support on transformation products analysis in ProVIS, and thank Dr. Matthias Gehre for his help in the Isotope Laboratory of the UFZ. We are grateful to Axel Horst for critical reading of our manuscript.

Conflicts of interest: none.

References

Bacaloni, A., Cucci, F., Guarino, C., Nazzari, M., Samperi, R., Laganà, A., 2008. Occurrence of organophosphorus flame retardant and plasticizers in three volcanic lakes of central Italy. Environ. Sci. Technol. 42, 1898-1903.

Bergman, A., Ryden, A., Law, R.J., de Boer, J., Covaci, A., Alaee, M., Birnbaum, L., Petreas, M., Rose, M., Sakai, S., Van den Eede, N., van der Veen, I., 2012. A novel abbreviation standard for organobromine, organochlorine and organophosphorus flame retardants and some characteristics of the chemicals. Environ. Int. 49, 57-82.

Berne, C., Allainmat, B., Garcia, D., 2005. Tributyl phosphate degradation by Rhodopseudomonas palustris and other photosynthetic bacteria. Biotechnol. Lett. 27, 561-566.

Blumenthal, E., Herbert, J., 1945. The mechanism of the hydrolysis of trimethyl orthophosphate. Trans. Faraday Soc. 41, 611-617.

Bouchard, D., Hunkeler, D., Höhener, P., 2008. Carbon isotope fractionation during aerobic biodegradation of n-alkanes and aromatic compounds in unsaturated sand. Org. Geochem. 39, 23-33.

Buxton, G.V., Greenstock, C.L., Helman, W.P., Ross, A.B., 1988. Critical review of rate constants for reactions of hydrated electrons, hydrogen atoms and hydroxyl radicals (·OH/·O−) in aqueous solution. J. Phys. Chem. Ref. Data 17, 513-886.

Coplen, T.B., 1996. New guidelines for reporting stable hydrogen, carbon, and oxygen isotope-ratio data. Geochim. Cosmochim. Acta 60, 3359-3360.

Day, J.N.E., Ingold, C.K., 1941. Mechanism and kinetics of carboxylic ester hydrolysis and carboxyl esterification. Trans. Faraday Soc. 1941, 686-705.

Elsner, M., 2010. Stable isotope fractionation to investigate natural transformation mechanisms of organic contaminants: principles, prospects and limitations. J. Environ. Monit. 12, 2005-2031.

Elsner, M., Zwank, L., Hunkeler, D., Schwarzenbach, R.P., 2005. A new concept linking observable stable isotope fractionation to transformation pathways of organic pollutants. Environ. Sci. Technol. 39, 6896-6916.

Fries, E., Püttmann, W., 2003. Monitoring of the three organophosphate esters TBP, TCEP and TBEP in river water and ground water (Oder, Germany). J. Environ. Monit. 5, 346-352.

Gray, J.R., Lacrampe-Couloume, G., Gandhi, D., Scow, K.M., Wilson, R.D., Mackay, D.M., Sherwood Lollar, B., 2002. Carbon and hydrogen isotopic fractionation during biodegradation of methyl tert-butyl ether. Environ. Sci. Technol. 36, 1931-1938.

Greget, R., Dadak, S., Barbier, L., Lauga, F., Linossier-Pierre, S., Pernot, F., Legendre, A., Ambert, N., Bouteiller, J.M., Dorandeu, F., Bischoff, S., Baudry, M., Fagni, L., Moussaoui, S., 2016. Modeling and simulation of organophosphate-induced neurotoxicity: Prediction and validation by experimental studies. Neurotoxicology 54, 140-152.

He, X., Mezyk, S.P., Michael, I., Fatta-Kassinos, D., Dionysiou, D.D., 2014. Degradation kinetics and mechanism of beta-lactam antibiotics by the activation of H2O2 and Na2S2O8 under UV-254nm irradiation. J. Hazard. Mater. 279, 375-383.

Herrmann, H., 2003. Kinetics of aqueous phase reactions relevant for atmospheric chemistry. Chem. Rev. 103, 4691-4716.

Herrmann, H., 2007. On the photolysis of simple anions and neutral molecules as sources of O-/OH, SOx- and Cl in aqueous solution. Phys. Chem. Chem. Phys. 9, 3935-3964.

Herrmann, H., Reese, A., Zellner, R., 1995. Time-resolved UV/VIS diode array absorption spectroscopy of SOx−(x=3, 4, 5) radical anions in aqueous solution. J. Mol. Struct. 348, 183-186.

House, D.A., 1962. Kinetics and Mechanism of Oxidations by Peroxydisulfate. Chem. Rev. 62, 185-&.

Kirby, A.J., Mora, J.R., Nome, F., 2013. New light on phosphate transfer from triesters. Biochim. Biophys. Acta. 1834, 454-463.

Lau, T.K., Chu, W., Graham, N.J., 2007. The aqueous degradation of butylated hydroxyanisole by UV/S2O82-: study of reaction mechanisms via dimerization and mineralization. Environ. Sci. Technol. 41, 613-619.

Lee, S., Jeong, W., Kannan, K., Moon, H.B., 2016. Occurrence and exposure assessment of organophosphate flame retardants (OPFRs) through the consumption of drinking water in Korea. Water Res. 103, 182-188.

Liang, C., Su, H.-W., 2009. Identification of sulfate and hydroxyl radicals in thermally activated persulfate. Ind. Eng. Chem. Res. 48, 5558-5562.

Martinez-Carballo, E., Gonzalez-Barreiro, C., Sitka, A., Scharf, S., Gans, O., 2007. Determination of selected organophosphate esters in the aquatic environment of Austria. Sci. Total Environ. 388, 290-299.

Mincher, B.J., Mezyk, S.P., Martin, L.R., 2008. A pulse radiolysis investigation of the reactions of tributyl phosphate with the radical products of aqueous nitric acid irradiation. J. Phys. Chem. A 112, 6275-6280.

Nancharaiah, Y.V., Reddy, G.K.K., Mohan, T.V.K., Venugopalan, V.P., 2015. Biodegradation of tributyl phosphate, an organosphate triester, by aerobic granular biofilms. J. Hazard. Mater. 283, 705-711.

Neta, P., Huie, R.E., Ross, A.B., 1988. Rate constants for reactions of inorganic radicals in aqueous solution. J. Phys. Chem. Ref. Data 17, 1027-1284.

Nijenhuis, I., Richnow, H.H., 2016. Stable isotope fractionation concepts for characterizing biotransformation of organohalides. Curr. Opin. Biotechnol. 41, 108-113.

Northrop, D.B., 1981. The expression of isotope effects on enzyme-catalyzed reactions. Annual review of biochemistry 50, 103-131.

Oh, Y.-C., Bao, Y., Jenks, W.S., 2003. Isotope studies of photocatalysis: TiO2-mediated degradation of dimethyl phenylphosphonate. J. Photoch. Photobio. A: Chem 161, 69-77.

Ou, H.s., Liu, J., Ye, J.s., Wang, L.l., Gao, N.y., Ke, J., 2017. Degradation of tris(2-chloroethyl) phosphate by ultraviolet-persulfate: Kinetics, pathway and intermediate impact on proteome of Escherichia coli. Chem. Eng. J. 308, 386-395.

Paneth, P., Buncel, E., Saunders Jr, W., 1992. Isotopes in Organic Chemistry Vol. 8. Elsevier, New York.

Rayleigh, L., 1896. L.Theoretical considerations respecting the separation of gases by diffusion and similar processes. Philos. Mag. 42, 493-498.

Regnery, J., Puttmann, W., 2010. Occurrence and fate of organophosphorus flame retardants and plasticizers in urban and remote surface waters in Germany. Water Res.

44, 4097-4104.

Regnery, J., Puttmann, W., Merz, C., Berthold, G., 2011. Occurrence and distribution of organophosphorus flame retardants and plasticizers in anthropogenically affected groundwater. J. Environ. Monit. 13, 347-354.

Rodil, R., Quintana, J.B., Concha-Grana, E., Lopez-Mahia, P., Muniategui-Lorenzo, S., Prada-Rodriguez, D., 2012. Emerging pollutants in sewage, surface and drinking water in Galicia (NW Spain). Chemosphere 86, 1040-1049.

Russell, G.A., 1957. Deuterium-isotope effects in the autoxidation of aralkyl hydrocarbons. Mechanism of the interaction of peroxy radicals. J. Am. Chem. Soc. 79, 3871-3877.

Shi, Y., Gao, L., Li, W., Wang, Y., Liu, J., Cai, Y., 2016. Occurrence, distribution and seasonal variation of organophosphate flame retardants and plasticizers in urban surface water in Beijing, China. Environ. Pollut. 209, 1-10.

Su, G., Letcher, R.J., Yu, H., 2016. Organophosphate Flame Retardants and Plasticizers in Aqueous Solution: pH-Dependent Hydrolysis, Kinetics, and Pathways. Environ. Sci. Technol. 50, 8103-8111.

Thullner, M., Centler, F., Richnow, H.-H., Fischer, A., 2012. Quantification of organic pollutant degradation in contaminated aquifers using compound specific stable isotope analysis – Review of recent developments. Org. Geochem. 42, 1440-1460.

Van Breukelen, B.M., 2007. Extending the Rayleigh equation to allow competing isotope fractionating pathways to improve quantification of biodegradation. Environ. Sci. Technol. 41, 4004-4010.

Vogt, C., Dorer, C., Musat, F., Richnow, H.H., 2016. Multi-element isotope fractionation concepts to characterize the biodegradation of hydrocarbons - from enzymes to the environment. Curr. Opin. Biotechnol. 41, 90-98.

Waclawek, S., Lutze, H.V., Grubel, K., Padil, V.V.T., Cernik, M., Dionysiou, D.D., 2017. Chemistry of persulfates in water and wastewater treatment: A review. Chem. Eng. J. 330, 44-62.

Wanamaker, E.C., Chingas, G.C., McDougal, O.M., 2013. Parathion hydrolysis revisited: in situ aqueous kinetics by 1H NMR. Environ. Sci. Technol. 47, 9267-9273.

Watts, M.J., Linden, K.G., 2009. Advanced oxidation kinetics of aqueous tri alkyl phosphate flame retardants and plasticizers. Environ. Sci. Technol. 8, 2937-2942.

Watts, R.J., Teel, A.L., 2006. Treatment of contaminated soils and groundwater using ISCO. Practice Periodical of Hazardous, Toxic, and Radioactive Waste Management 10, 2-9.

Wolfsberg, M., Van Hook, W.A., Paneth, P., Rebelo, L.P.N., 2009. Isotope effects: in the chemical, geological, and bio sciences. Springer Science & Business Media.

Wu, L., Chládková, B., Lechtenfeld, O.J., Lian, S., Schindelka, J., Herrmann, H., Richnow, H.H., 2018a. Characterizing chemical transformation of organophosphorus compounds by 13C and 2H stable isotope analysis. Sci. Total Environ. 615, 20-28.

Wu, L., Kummel, S., Richnow, H.H., 2017. Validation of GC-IRMS techniques for δ13C and δ2H CSIA of organophosphorus compounds and their potential for studying the mode of hydrolysis in the environment. Anal. Bioanal. Chem. 409, 2581-2590.

Wu, L., Verma, D., Bondgaard, M., Melvej, A., Vogt, C., Subudhi, S., Richnow, H.H., 2018b. Carbon and hydrogen isotope analysis of parathion for characterizing its natural attenuation by hydrolysis at a contaminated site. Water Res. 143, 146-154.

Wu, L., Yao, J., Trebse, P., Zhang, N., Richnow, H.H., 2014. Compound specific isotope analysis of organophosphorus pesticides. Chemosphere 111, 458-463.

Wu, T., Gan, Q., Jans, U., 2006. Nucleophilic substitution of phosphorothionate ester pesticides with bisulfide (HS-) and polysulfides (Sn2-). Environ. Sci. Technol. 40, 5428-5434.

Yang, Y., Lu, X., Jiang, J., Ma, J., Liu, G., Cao, Y., Liu, W., Li, J., Pang, S., Kong, X., Luo, C., 2017. Degradation of sulfamethoxazole by UV, UV/H2O2 and UV/persulfate (PDS): Formation of oxidation products and effect of bicarbonate. Water Res. 118, 196-207.

Zhang, N., Geronimo, I., Paneth, P., Schindelka, J., Schaefer, T., Herrmann, H., Vogt, C., Richnow, H.H., 2016. Analyzing sites of OH radical attack (ring vs. side chain) in oxidation of substituted benzenes via dual stable isotope analysis (δ13C and δ2H). Sci. Total Environ. 542, 484-494.

***Highlights (3 to 5 bullet points (maximum 85 characters including spaces per bullet point)**

Highlights

1. Quantification of ^{2}H and ^{13}C isotope enrichment factors of TBP

2. Comparison of isotope fractionation patterns upon hydrolysis and radical oxidation

3. Characterization of the C-O and C-H bond cleavage of TBP using AKIE

Carbon and hydrogen stable isotope analysis for characterizing the chemical degradation of tributyl phosphate

Jia Liu[1,2 §], Langping Wu[2 §], Steffen Kümmel[2], Jun Yao[3], Thomas Schaefer[4], Hartmut Herrmann[4], Hans-Hermann Richnow[2,3*]

[1]School of Energy and Environmental Engineering, University of Science and Technology Beijing, Xueyuan Road No.30, Haidian District, Beijing 100083, PR China

[2]Department of Isotope Biogeochemistry, Helmholtz Centre for Environmental Research-UFZ, Permoserstraße15, Leipzig 04318, Germany

[3]School of Water Resources and Environment, China University of Geosciences (Beijing), Xueyuan Road No.29, Haidian District, Beijing 100083, PR China

[4]Atmospheric Chemistry Department (ACD), Leibniz Institute for Tropospheric Research (TROPOS), Permoserstraße15, Leipzig 04318, Germany

§ Dual-first authorship: the two authors have contributed equally to this work.

* To whom correspondence should be addressed:

E-mail: hans.richnow@ufz.de Tel.: +49 (0) 341 235 1212, Fax: +49 (0) 341 2351443

Abstract

Tributyl phosphate (TBP) belongs to the group of trialkyl substituted organophosphate esters. Its chemical reactivity depends on the stability of various chemical bonds. TBP was used as a model compound for the development of a concept using stable isotope fractionation associated with bond cleavage reactions for better understanding the fate of TBP in the environment. Carbon isotope enrichment factors (ε_C) of TBP hydrolysis were found to be pH dependent (-3.8 ± 0.3‰ at pH 2, -4.6 ± 0.5‰ at pH 7, -2.8 ± 0.1‰ at pH 9, no isotope fractionation at pH 12), which is in accordance with the mode of a S_N2 hydrolytic bond cleavage. Hydrogen isotope fractionation was negligible as no H bond cleavage is involved during hydrolysis. The apparent carbon kinetic isotope effect ($AKIE_C$) ranged from 1.045 to 1.058. In contrast to hydrolysis, both carbon and hydrogen isotope fractionation were observed during radical oxidation of TBP by $^{\bullet}OH$ and $SO_4^{\bullet-}$, yielding ε_C from -0.9 ± 0.1‰ to -0.5 ± 0.1‰ and ε_H from -20 ± 2‰ to -11 ± 1‰. $AKIE_C$ and $AKIE_H$ varied from 1.007 to 1.011 and from 1.594 to 2.174, respectively. The correlation of ^{2}H and ^{13}C fractionation revealed Λ values ranging from 17 ± 1 to 25 ± 6. Results demonstrated that the correlation of ^{2}H and ^{13}C isotope fractionation of TBP allowed to identify radical reactions and to distinguish them from hydrolysis. The presented dual isotope analysis approach has diagnostic value for characterizing the chemical transformation of TBP in the environment.

Keywords

tributyl phosphate, isotope fractionation, hydrolysis, radical oxidation, AKIE

1. Introduction

Tributyl phosphate (TBP) is an organophosphorus compound widely used as flame retardant, plasticiser, anti-foamer, component of herbicides and hydraulic fluids (Regnery et al., 2011). In addition, it was extensively used as a solvent for plutonium uranium redox extraction (PUREX) for nuclear fuel reprocessing (Mincher et al., 2008). The production of commercially used TBP is about 3000-5000 tons/year in Europe (Nancharaiah et al., 2015). Due to its extensive use, TBP is frequently detected in the aquatic environment of many countries, including Germany (Fries and Püttmann, 2003; Regnery and Puttmann, 2010), Austria (Martinez-Carballo et al., 2007), Italy (Bacaloni et al., 2008), Spain (Rodil et al., 2012), Korea (Lee et al., 2016), and China (He et al., 2014; Shi et al., 2016).

TBP can inhibit the enzyme acetylcholine esterase (AChE), resulting in cholinergic toxicity of the autonomic system and can thus lead to respiratory paralysis and even death (Bergman et al., 2012; Greget et al., 2016). Given these adverse effects, TBP has been an environmental concern for decades, especially in aquatic systems. The main degradation pathways are hydrolysis, indirect photo-oxidation or microbial degradation (Berne et al., 2005; Watts and Linden, 2009; Nancharaiah et al., 2015; Su et al., 2016). These are probably the key processes how TBP is degraded or attenuated in the environment. Direct chemical oxidation is effective for the removal of organic contaminants in waste water. In particular, chemicals, such as hydrogen peroxide, persulfate, permanganate and ozone, have been applied for in situ chemical oxidation (ISCO) for the treatment of subsurface TBP or similar contamination (Watts and Teel, 2006). Hydroxyl radicals ($^{\bullet}$OH) are an effective oxidant with redox potential of 1.7–2.8 V and are frequently used for wastewater remediation (Waclawek et al., 2017). Similar to $^{\bullet}OH$, the sulfate radical ($SO_4^{\bullet-}$) with a redox potential of 2.5–3.1 V is efficient for the oxidation of many organic compounds (Neta et al., 1988). $SO_4^{\bullet-}$ can be generated for example from peroxydisulfate ($S_2O_8^{2-}$, PS) or peroxymonosulfate ($HS_2O_5^{-}$) salts by the activation of the persulfate anion ($S_2O_8^{2-}$, $E_0 = 2.01$ V) using light (Herrmann, 2007; Yang et al., 2017) or heat (House, 1962; Liang and Su, 2009). Over the past ten years, considerable attention has been paid to potassium peroxydisulfate (KPS) because of its lower cost compared to H_2O_2 or O_3 and the high efficiency for organic mineralization (Lau et al., 2007; Waclawek et al., 2017).

Conventionally, degradation pathways are chemically analysed by measuring the concentrations decrease of reactants and the appearance of degradation products for the identification of reaction products. However, this approach often has large uncertainties because of the influence of physical processes (such as dilution, volatility and sorption), the challenges of detecting unknown products and the difficulties to establish mass balances. As an alternative technology, compound specific isotope analysis (CSIA) making use of isotope fractionation processes of degradation reactions can be used for the qualitative characterisation and quantitative estimation of processes involved in organic compound degradation in the environment. This technique is becoming a routine and practical approach in biogeochemistry and environmental science (Elsner, 2010; Thullner et al., 2012; Nijenhuis and Richnow, 2016; Vogt et al., 2016).

For better understanding of the transformation mechanisms, the kinetic isotope effect (KIE) based on chemical bond change reactions can be analyzed. The KIE characterizes the rate limitation of a bond change reaction posed by isotopologues. The rate limitation is equivalent to the stability of heavy and light isotope substituted bonds and characterizes the transition state of a chemical reaction (Northrop, 1981; Wolfsberg et al., 2009). The apparent kinetic isotope effect (AKIE) can be calculated to normalize the isotope enrichment factor (ε) for non-reacting positions and intermolecular competition to compensate for "dilution" of the isotope composition in reacting isotopologues. The AKIE can be used to compare the kinetic isotope effect of bond cleavage reactions of different molecules. Multi-element isotope fractionation analysis correlating the isotope fractionation of two (or more) elements can be used to evaluate the degradation pathways (Gray et al., 2002; Elsner et al., 2005). Previous studies demonstrated the potential use of stable isotope fractionation for characterizing the transformation mechanisms of organophosphorus compounds, such as dichlorvos, dimethoate, methyl parathion, parathion and tris(2-chloroethyl) phosphate (Wu et al., 2014; Wu et al., 2017; Wu et al., 2018a).

In the present study, we systematically examined the carbon and hydrogen isotope fractionation upon hydrolysis of TBP under acidic, neutral and alkaline conditions to characterize the reaction pathways. The isotope fractionation patterns of TBP by radical oxidation ($SO_4^{\bullet-}$ and $^{\bullet}OH$) were also examined. The objectives of this study were to (1) investigate the kinetic reaction rate constant k_{obs} of hydrolysis and radical oxidation; (2) characterize the stable carbon and hydrogen isotope fractionation of TBP during hydrolysis and radical oxidation; (3) distinguish different mechanisms by using the AKIE values and correlating ^{2}H and ^{13}C isotope fractionation to obtain Λ values, which may be used diagnostically for tracing TBP degradation in the field.

2. Materials and methods

A detailed description of the analytical methods is provided in the Supplementary Information (SI).

2.1 Chemicals

All chemicals were of analytical grade quality and used without further purification. Tributyl phosphate (TBP, 99% purity) and dibutyl phthalate (DBP, >99% purity) were purchased from Xiya Company (China). Dichloromethane (DCM) was supplied by Carl Roth GmbH + Co. KG (Karlsruhe, Germany). Potassium peroxydisulfate ($K_2S_2O_8$), hydrogen peroxide (30% H_2O_2), di-potassium hydrogen phosphate (K_2HPO_4), potassium dihydrogen phosphate (KH_2PO_4), sodium hydrogen carbonate ($NaHCO_3$), sodium hydrate (NaOH), and disodium hydrogen phosphate (Na_2HPO_4) were supplied by Merck (Guaranteed reagent quality, Darmstadt, Germany). Solutions and pH buffers were prepared in ultrapure water obtained by a Milli-Q System (Millipore GmbH, Germany).

2.2 Hydrolysis and radical oxidation experiments

The following buffer solutions were used to obtain hydrolysis at different pH conditions: KCl-HCl (50 mM for pH 2), K_2HPO_4-KH_2PO_4 (100 mM for pH 7), $NaHCO_3$-NaOH (45.5 mM for pH 9), and Na_2HPO_4- NaOH (32.5 mM for pH 12).

Hydrolysis experiments: TBP is hydrolyzed with very slow reaction rates at room temperature under neutral to acidic conditions but rapidly hydrolyzed under strong alkaline condition (Su et al., 2016). In order to adjust the hydrolysis rates in the same order of magnitude for a better comparison of the isotope fractionation patterns associated with different reaction pathways, hydrolysis experiments were carried out at 80 °C to accelerate the hydrolysis rate at pH 2, pH 7 and pH 9, respectively. Hydrolysis experiments at pH 12 were performed at 35 °C to slow down the reaction. All experiments were conducted in 40 mL buffer solutions in 150-mL serum bottles with 100 mg L^{-1} TBP as initial concentration. At different time intervals, the reaction solutions were extracted by adding 1 mL DCM containing 1000 mg L^{-1} DBP as internal standard and shaking for at least 4 h at 10 °C. Extracts were stored at 4 °C prior to analysis. The extraction recovery and effect of the extraction procedure on carbon and hydrogen isotope signature were evaluated as described in Section 3 of the Supplementary Information.

Potassium peroxydisulfate (KPS) oxidation: For KPS oxidation experiments a molar ratio of TBP to KPS of 1:20 was used. The KPS oxidation reaction was not conducted at pH 2 due to the exclusive formation of secondary radicals and complicating subsequent reactions. At pH 2, the $SO_4^{\bullet-}$ reacts exclusively with the Cl^- from the HCl/ KCl buffer to produce a Cl atom, which will subsequently react to form $Cl_2^{\bullet-}$, a dichloride radical anion (Herrmann, 2003). Therefore, the KPS oxidation reactions were only conducted at pH 7, pH 9 and pH 12, respectively. The initial concentration of TBP was 100 ppm. Buffer solutions with different pH values were prepared as described above. All KPS oxidation reactions were carried out at 35 °C. Control experiments were carried out without the addition of KPS. Remaining TBP was extracted and analyzed as described in the hydrolysis experiment.

UV/H_2O_2 oxidation experiment: Photolysis experiments were carried out at pH 7 in phosphate buffer with 200 mg L^{-1} initial TBP concentration. Irradiation was achieved by

150 W xenon lamp (Type no. L2175, Hamamatsu, Japan), which covered a broad continuous spectrum from 185 nm to 2000 nm. A long-pass filter with a cut-off of short UV wavelengths below 280 nm (20CGA-280, Newport Corporation, Irvine, U.S.) was applied. Direct photolysis is not expected at the applied UV wavelengths due to the almost negligible photon absorption by TBP (Watts and Linden, 2009). The molar ratio of TBP to H_2O_2 was 1:5. In order to investigate the effects of buffer solution concentrations and reaction rates on the isotope fractionation of TBP, three experiments were carried out in 100 mM buffer solution at 20 °C (UV/H_2O_2_1), 100 mM buffer solution at 15 °C (UV/H_2O_2_2) and 10 mM buffer solution at 15 °C (UV/H_2O_2_3), respectively. 100 mM buffer solution was applied to make sure that the pH will remain stable at 7 during the reaction. Lower buffer concentration of 10 mM was applied to minimize the formation of the secondary radicals (SI, section 5). The experiments were conducted at different temperature of 20 °C and 15 °C to slow down the reaction rate. For direct photolysis, experiments were conducted under the same conditions but without the addition of H_2O_2 in a 100 mM buffer solution at 20 °C. Dark control experiments were conducted under identical experimental conditions without UV exposure (100 mM buffer solution). More information on the experimental setup of the UV degradation experiments are described elsewhere (Zhang et al., 2016). The transformation products of TBP in UV/H_2O_2 experiments were tentatively analyzed by a Fourier-transform ion cyclotron resonance mass spectrometer (FT-ICR MS, Solarix XR 12T, Bruker Daltonics), the analytical procedures were described in SI.

2.3 Data analysis

Isotope ratios were expressed as delta notation ($\delta^{h}E$) in parts per thousand (‰) based on Eq. [1]. Here, R_{sample} is the ratio of the heavy (^{h}E) to the light isotopes (^{l}E) of a sample and R_{ref} corresponds to the ratio of the respective isotopes of reference. For stable carbon isotope analyses the Vienna Pee Dee Belemnite (V-PDB) is used as reference, whereas for stable hydrogen isotope analyses the Vienna Standard Mean Ocean Water (V-SMOW) is applied (Coplen, 1996).

$$\delta\,^{h}\mathrm{E} = \left(\frac{\mathrm{R}_{sample}}{\mathrm{R}_{ref}} - 1\right) = \left(\frac{^{h}\mathrm{E}/\,^{l}\mathrm{E}}{^{h}\mathrm{E}_{ref}/\,^{l}\mathrm{E}_{ref}} - 1\right) \qquad [1]$$

The isotope enrichment factor (ε_E) can be determined from the logarithmic form of the Rayleigh equation, as shown in Eq. [2] (Rayleigh, 1896; Elsner, 2010). The variables $\delta^{h}E_t$ and $\delta^{h}E_0$ are the isotope compositions of a compound for the element E at time t and time zero, respectively, and *f* is the residual substrate fraction. The changes in concentration during the reaction (C_t/C_0) can be related to the changes in isotope composition by ε_E.

$$\ln\left(\frac{\delta^{h}\mathrm{E}_t+1}{\delta^{h}\mathrm{E}_0+1}\right) = \varepsilon_E \cdot \ln f = \varepsilon_E \cdot \ln\left(\frac{\mathrm{C}_t}{\mathrm{C}_0}\right) \qquad [2]$$

The $\mathrm{AKIE_E}$ value of the bond cleavage at the reactive position can be calculated with Eq. [3], where n is the total number of atoms for element E in the molecule, x is the number of reactive sites, and z is the number of indistinguishable reactive sites (Elsner et al., 2005). The normalisation of $\mathrm{AKIE_E}$ corrects the bulk isotope enrichment for non-reactive positions and the intramolecular isotopic competition.

$$\mathrm{AKIE} = \frac{1}{1 + \frac{n}{x} \times z \times \varepsilon} \qquad [3]$$

Assuming that two processes (process 1 and 2) are reacting with the same substrate simultaneously and both processes follow first-order kinetics, the contribution of the individual processes in the mixed reaction can be estimated by an extended Rayleigh-type equation using the individual isotope enrichment factors of the particular reaction (ε_1 and ε_2). The observable ε_i of the mixed reaction and the ε_1 and ε_2 of the individual pathway 1 and 2 are needed for this calculation. The rate ratio of two competing degradation pathways (F) can be calculated by Eq. (4) (Van Breukelen, 2007), indicating the isotope fractionation contributed by pathway 1 to the observed ε_i.

$$F = \frac{\varepsilon_i - \varepsilon_2}{\varepsilon_1 - \varepsilon_2} \qquad [4]$$

3. Results

3.1 Effects of extraction on isotope signature

The recovery of the liquid/liquid DCM extraction method was 91.2 ± 10.2% (Fig. S2 (a)). The isotope shifts of TBP before and after DCM extraction were 0.05 – 0.65‰ for $\delta^{13}C$, and 1 – 4‰ for $\delta^{2}H$ (Fig. S2 (b)), respectively. Considering the analytical uncertainty of carbon and hydrogen isotope compositions, which is < ±0.5‰ and < ±5‰ for carbon and hydrogen, respectively, carbon and hydrogen isotope shifts due to the extraction process are insignificant. A detailed description was provided in SI, section 3.

3.2 Isotope fractionation of TBP during hydrolysis

The degradation curves and changes in carbon and hydrogen isotope compositions of TBP are illustrated in Fig. 1, and the obtained k_{obs} and ε values for TBP hydrolysis are summarized in Table 1. All hydrolysis experiments followed pseudo-first order kinetics with R^2 better than 0.97, alkaline conditions resulted in higher reaction rates compared to neutral and acidic conditions (pH 12 > pH 9 > pH 7 ≈ pH 2) (Table 1). The stable carbon isotope enrichment could be quantified by the Rayleigh equation. At pH 2, 90% degradation was achieved within 1236 h, resulting in a carbon enrichment factor (ε_C) of -3.8 ± 0.3‰. 88% degradation was achieved within 1140 h at pH 7, yielding an ε_C of -4.6 ± 0.5‰. 94% degradation was achieved within 864 h and yielding an ε_C of -2.8 ± 0.1‰ at pH 9. At pH 12, 80% degradation was achieved after 1464 h and no carbon enrichment was observed. Hydrogen isotope fractionation was not observed in all hydrolysis experiments (Fig. 1).

3.3 Isotope fractionation of TBP during KPS oxidation

The degradation curves and changes in carbon and hydrogen isotope compositions of TBP are illustrated in Fig. 2, and the corresponding k_{obs} and ε values are summarized in Table 1. All oxidation experiments followed pseudo-first order kinetics and the k_{obs} values decreased with increasing pH (Table 1). The stable carbon and hydrogen isotope fractionation could be quantified by the Rayleigh equation. About 95% TBP was degraded within 292 h at pH7/KPS, resulting in a ε_C = -0.9 ± 0.1‰ and ε_H = -16 ± 2‰, respectively. At pH9/KPS, 95% degradation was achieved within 332 h, yielding an ε_C of -0.8 ± 0.1‰ and an ε_H of -20 ± 2‰. At pH12/KPS, TBP was depleted to 90% within 400 h, corresponding to an ε_C = -0.5 ± 0.1‰ and ε_H = -11 ± 1‰. No degradation took place in control experiments except for pH12/KPS (Fig. S2). Due to the hydrolysis at pH 12, 35% of TBP was degraded within 400 h.

3.4 Isotope fractionation of TBP during UV/H_2O_2 oxidation

Degradation curves and changes in carbon and hydrogen isotope compositions of TBP are illustrated in Fig. 2. All experiments followed pseudo-first order kinetics, and the k_{obs} values (× 10^{-3} h^{-1}) were 474.2 ± 11.4 in UV/H_2O_2_1, 27.9 ± 2.4 in UV/H_2O_2_2 and 6.8 ±

0.5 in UV/H_2O_2_3, respectively (Table 1). All coefficients of determination (R^2) were larger than 0.99. In the experiment UV/H_2O_2_1, 96% TBP was degraded within 6.7 h, yielding a ε_C of -0.8 ± 0.1‰ and ε_H of -14 ± 1‰. In the degradation experiment UV/H_2O_2_2, 85% TBP was depleted in 72.5 h, resulting in a ε_C of -0.6 ± 0.3‰ and ε_H of -13 ± 3‰. In the degradation experiment UV/H_2O_2_3, 93% TBP was transformed within 385 h, and an ε_C of -0.6 ± 0.2‰ and ε_H of -17 ± 7‰ were obtained. In the control experiment without H_2O_2 employing the conditions used in UV/H_2O_2_1, no significant change of the TBP concentration was observed (Fig.S2 d), suggesting that direct photolysis did not take place during these experiments.

3.5 Analysis of transformation products of TBP in the UV/H_2O_2 experiment

Three potential transformation products were tentatively characterized as di-n-butylphosphate (P1), keto-tri-butylphosphate (P2), and hydroxy-tri-butylphosphate (P3) (Table S1 and Fig. S3). The detailed information of characterized transformation products is given in the SI, section 7. The precise position of the hydroxyl or keto group at the side chain of the TBP molecule could not be confirmed, however, it is likely that the functional group is formed by radical attack at the sub-terminal carbon of the butyl chain.

3.6 Two dimensional isotope fractionation (C-H)

In order to explore the diagnostic potential of two dimensional isotope fractionation analysis, the hydrogen and carbon isotope fractionation were plotted to obtain Λ values ($\Lambda = \frac{\Delta\,^2H}{\Delta^{13}C} \approx \frac{\varepsilon_H}{\varepsilon_C}$, $\Delta^{13}C = \delta_t{}^{13}C - \delta_0{}^{13}C$, $\Delta^2H = \delta_t{}^2H - \delta_0{}^2H$). However, due to the absence of hydrogen isotope fractionation Λ could not be defined for hydrolysis. In contrast, the radical oxidation of TBP under pH7/KPS, pH9/KPS and pH12/KPS conditions resulted in Λ values of 17 ± 1, 23 ± 1, 19 ± 1, respectively (Table 1). The reactions of TBP by

UV/H_2O_2 (dominant $^{\bullet}OH$ reaction, described in SI, section 5) yielded an average Λ value of 20 ± 4 (Table 1), which is statistically identical with the ones obtained from KPS oxidation experiments. The two dimensional isotope fractionation analysis of all radical oxidation experiments including $SO_4^{\bullet-}$ and $^{\bullet}OH$ gave an average Λ value of 20 ± 4 (Table 1).

4. Discussion

4.1 Insight of the isotope fractionation during hydrolysis

A previous study proposed two hydrolysis pathways of organophosphorus compounds (OPs) (Fig. 3a,b): the first one is OH^- or H_2O attacks the phosphorus atom; the second one is H_2O attacks the carbon atom (Wu et al., 2006). The acid-catalysed hydrolysis of esters mainly proceeds via an $A_{AC}2$ mechanism suggesting an acyl-oxygen fission (AC) in a bimolecular reaction (Day and Ingold, 1941). For instance, under acidic and neutral conditions, trimethyl phosphate may lead to a C–O bond split as demonstrated in experiments with ^{18}O-labelled water as indicator (Blumenthal and Herbert, 1945). Consequently, the C-O bond cleavage leads to carbon isotope fractionation of TBP. At high pH (e.g., pH >10), OH^- attacks the phosphorus atom through simple nucleophile displacement (S_N2-type) leading to a P–O bond cleavage (Wanamaker et al., 2013). The reaction may proceed via a two-step addition-elimination pathway involving a pentacoordinate intermediate, such as TS1 and TS2 (Fig. 3b) (Kirby et al., 2013). The observed negligible carbon and hydrogen isotope fractionation of TBP at pH 12 highly supports a P–O bond split.

At pH 9, the observed carbon isotope fractionation of TBP provided evidence for a C–O bond split. However, the ε_C value at pH 9 was lower than that of pH 2 and pH 7. The same phenomenon was observed during methyl parathion and ethyl parathion hydrolysis (Wu et al., 2018a). Given that hydrolysis of OPs is pH dependent, no precise pH boundary can be used for the identification of C–O or P–O bond split. The two major degradation pathways occurred simultaneously at pH 9. The P–O bond cleavage is not associated with carbon isotope fractionation, and thus carbon isotope fractionation can be solely attributed to the splitting of the C–O bond. Considering that the carbon fractionation observed in experiments for acid hydrolysis (pH 2) and alkaline hydrolysis (pH 12) are representative for the mechanism for C–O and P–O bond split respectively, and both processes follow the first-order kinetics, Eq. [4] can be applied for the calculation of the contribution of the two pathways acting during the hydrolysis at pH 9. The carbon isotope enrichment factors of hydrolysis at pH 2 (ε_1 = -3.8 ± 0.3‰) and the ε_2 value of 0‰ representing hydrolysis at pH 12 were used for calculation. Within the uncertainty of isotope enrichment factors observed in the experiments, the enrichment factor of TBP at pH 9 (ε_i = -2.8±0.1‰) suggests that 67–80% of TBP was hydrolysed via the C–O bond cleavage pathway, and the remaining 20–33% was attributed to the P–O bond split. The mechanism of acidic and neutral hydrolysis is almost identical, and the calculation is also valid for comparing contributions at neutral conditions.

For testing the hypothesis of the degradation mechanisms the AKIE values were compared to intrinsic KIE reactions. For TBP hydrolysis, $\mathrm{AKIE_C}$ (calculation is described in SI, section 6) ranged from 1.048 to 1.058, which is in line with the intrinsic KIE values of nucleophilic substitution (1.03–1.09; S_N2 type on C–O bond) (Paneth et al., 1992), supporting the conclusion of C–O bond cleavage during TBP hydrolysis.

4.2 pH-dependency of radical oxidation

In this study, either $SO_4^{\bullet-}$ or $^{\bullet}OH$ was involved in persulfate oxidation, which is a pH-dependent reaction. Once $SO_4^{\bullet-}$ was generated by $S_2O_8^{2-}$ scission, it could propagate a chain of reactions involving the formation of other reactive species. $SO_4^{\bullet-}$ can react with water at all pH levels, forming $^{\bullet}OH$ (Eq. [S1]) (Neta et al., 1988; Herrmann et al., 1995). With the increase of pH, $SO_4^{\bullet-}$ preferentially reacts with OH^- forming $^{\bullet}OH$ with an increasing rate constant (Eq. [S2]) (Neta et al., 1988; Herrmann et al., 1995). Hence, at low pH (i.e. pH 7), $SO_4^{\bullet-}$ is the predominant reactive species, whereas at pH 9, both $SO_4^{\bullet-}$ and $^{\bullet}OH$ could coexist and at pH 12, $^{\bullet}OH$ is predominant (Liang and Su, 2009). Considering both radical species can be quenched to some extent by the PO_4^{3-} and CO_3^{2-} components in the buffer, the contributions of secondary radicals formed during the reaction and subsequent reaction with TBP were taken into account and the contributions were estimated to be minor (description in SI, section 5).

During radical oxidation of TBP, the rate constants have the following order: pH 7 > pH 9 > pH 12 (Table 1), demonstrating that the reaction can be retarded by increasing pH. The rate constants are associated with the reactivity of the radicals as $SO_4^{\bullet-}$ has a stronger redox potential than $^{\bullet}OH$ (Buxton et al., 1988; Neta et al., 1988), and thus may result in larger kinetic rate constants. The TBP oxidation by KPS at pH 12 had a 5 times larger rate constant compared to the hydrolysis at pH 12 (Table 1) suggesting that radical oxidation was dominating the degradation reaction. Nevertheless, two degradation processes co-existed in the degradation of TBP in the pH12/KPS system, namely, radical oxidation and alkaline hydrolysis. The contribution of alkaline hydrolysis on the TBP degradation was 35% based on the control experiment without the addition of KPS (Fig. S2).

4.3 Insight of isotope fractionation during $^{\bullet}OH$ and $SO_4^{\bullet-}$ reaction with TBP

$^{\bullet}OH$ which can be generated by H_2O_2 under UV irradiation has a high tendency to react non-selectively on functional groups via electron transfer, hydrogen abstraction or electrophilic/radical addition (Buxton et al., 1988). The transformation products formed in the UV/H_2O_2 reaction with TBP were tentatively identified as keto and hydroxylated derivatives (Table S1), suggesting a hydrogen abstraction from the alkyl chain at sub-terminal positions. This suggests a formation of a radical at the side chain which is quenched by oxygen forming a meta stable intermediate radical followed by a Russell mechanism (Russell, 1957) to form keto and hydroxyl TBP (Fig. 3c). In subsequent steps further reactions may lead to the formation of dibutyl phosphate. The hydrogen abstraction mechanism will lead to ^{2}H and ^{13}C isotope fractionation of TBP. Alternatively, radical addition, for example $^•$OH addition to the central phosphorus atom, may form a $(C_4H_9O)_3PO^•OH$ radical leading to elimination of butanol and resulting in dibutyl phosphate (Fig. 3c). However, $^•$OH addition to phosphate will lead to P-O cleavage and is unlikely to induce ^{2}H and ^{13}C isotope fractionation. Similar mechanisms have been observed in previous studies during the $^•$OH reaction with tri-(2chloroethyl) phosphate (Wu et al., 2018a) and dimethyl phenylphosphonate (Oh et al., 2003). According to the reaction mechanisms of $SO_4^{•-}$ and tri-(2chloroethyl) phosphate, $SO_4^{•-}$ was reported to react with phosphorus and carbon atoms, thereby causing a P–O and C–H bond split (Ou et al., 2017). Similarly, two pathways were proposed to be involved in TBP oxidation induced by $SO_4^{•-}$. One pathway involves the addition to the phosphorus centre and rupturing of $–OCH_2CH_2CH_2CH_3$ chains and the other one involves the addition to the $–CH_2–$ moieties causing the C–H bond split.

The radical reaction with the alkane side chain at the sub-terminal position cleaving a C-H bond in the transition state leads to ^{2}H and ^{13}C isotope fractionation. The observed ^{2}H and ^{13}C isotope fractionation in our experiments showed that this pathway took place during radical oxidation of TBP by $^•$OH and $SO_4^{•-}$. The obtained ε_C and ε_H at pH7/KPS ($SO_4^{•-}$ dominating) and pH9/KPS ($SO_4^{•-}$ and $^•$OH co-existing) were very similar with the ones from UV/H_2O_2 (pure $^•$OH) (Table 1). The slightly smaller ε_C of -0.5±0.1‰ and ε_H of -11±1‰

at pH12/KPS ($^{\bullet}$OH dominating) is due to the effect of alkaline hydrolysis of TBP at pH 12. Considering 35% of TBP degradation was contributed by alkaline hydrolysis (process 1) at pH12/KPS (Fig. S2), the ε associated with the $^{\bullet}$OH oxidation process (process 2) can be estimated using Eq. (4) where F = 0.35, ε_i = -0.5±0.1‰ for carbon and -11±1‰ for hydrogen, ε_1 = 0‰. Thus, ε_2 was calculated to be -0.8±0.2‰ for carbon and -17±2‰ for hydrogen, which were identical with the ones obtained from radical oxidation of TBP at pH7/KPS, pH9/KPS and UV/H_2O_2 conditions (Table 1). The average values of ε_C = -0.7±0.1‰, ε_H = -16±3‰, and Λ = 20±4 calculated from all individual radical oxidation experiments suggest that $SO_4^{\bullet-}$ and $^{\bullet}$OH radical oxidation processes of TBP could not be distinguished based on isotope enrichment factors within the uncertainty of our results, and it may suggest that both reaction processes had similar mechanisms of attacking carbon atoms and cleaving C–H bonds. However, P–O bond splitting cannot be characterized by the ^{2}H and ^{13}C isotope fractionation of TBP in this study, therefore, ^{2}H and ^{13}C isotope fractionation studies cannot provide direct evidence to evaluate the process of P–O bond cleavage.

The $AKIE_C$ which ranged from 1.007 to 1.011 for all radical oxidation experiments (Table 1) is consistent with those reported for *n*-alkanes' chemical transformation (1.01–1.02) (Bouchard et al., 2008) and lower than the Streitwieser Limits for a C–H bond (1.021) cleavage (Elsner et al., 2005). A series of studies yield $AKIE_H$ values between 2–23 that are typical for H-bond cleavage (Elsner et al., 2005). The $AKIE_H$ values reported in this study were lower and ranged from 1.608 to 2.174, indicating that steps other than the C–H bond cleavage were also rate-determining for radical oxidation of TBP. Potentially a radical reaction at the phosphate moiety may contribute to TBP degradation (Fig.3c 2) but do not contribute to ^{2}H and ^{13}C isotope fractionation. This may explain why the calculated AKIE values are lower than those typically expected for C-H bond cleavage. In our case the calculated AKIE values do not describe the KIE of the C-H bond cleavage at the side chain of TBP because the overall transformation reaction has a contribution of OH addition to the phosphate. However our current data do not allow validating this hypothesis in more detail.

4.4 Identification of degradation pathways by 2D-plot to analyse Λ values

The $SO_4^{\bullet-}$ and $^{\bullet}OH$ resulted in a characteristic isotope fractionation pattern (Λ values) for radical oxidation reactions of TBP. As hydrolysis did not lead to primary hydrogen isotope effects, hydrolysis and radical oxidation of TBP can be clearly distinguished by the correlation of ^{2}H and ^{13}C fractionation (Fig. 4). Similar results have been reported for radical oxidation of tris(2-chloroethyl) phosphate by $^{\bullet}OH$ formed in Fenton reactions and UV/H_2O_2 (Wu et al., 2018a). However, considering the obtained identical Λ values (section 3.5), the Λ values do not allow for separating the mechanisms of $SO_4^{\bullet-}$ and $^{\bullet}OH$ reactions with TBP. The Λ values are not affected when non-isotope-fractionating processes such as alkaline hydrolysis are influencing overall degradation, showing that mechanisms can also be identified when non-isotope-fractionating processes are at work. This may imply that the extent of isotope fractionation can be used for the assessment of radical reactions and may allow for the selection of an isotope enrichment factor representative for radical reactions. This isotope enrichment factor could then be used to calculate the contribution of degradation of TBP by radical reactions to the overall degradation in the environment. For example the hydrogen enrichment factor could be used to quantify the contribution of radical reactions because hydrolysis does not exhibit ^{2}H fractionation. The ^{2}H and ^{13}C isotope fractionation pattern of parathion has been used at an industrial dumpsite to characterise the contribution of neutral and acidic hydrolysis of parathion in a remediation measure (Wu et al., 2018b). Similarly, the Λ values determined throughout the current study could be used in the future to characterise degradation reaction in field studies for quantifying hydrolysis or chemical oxidation reactions. Further information for quantification of degradation reactions in the environment using enrichment factors have been summarised previously (Thullner et al., 2012).

5. Conclusions

In this study, the carbon and hydrogen isotope fractionation caused by hydrolysis and radical oxidation of TBP were systematically examined at different pH conditions. The $AKIE_C$ of the hydrolysis under neutral and acidic conditions was 1.048 - 1.058, which was consistent with an S_N2-type displacement reaction cleaving the C-O bond. At pH 12, a S_N2-type nucleophilic displacement reaction cleaving the P-O bond was characterized by the absence of carbon and hydrogen isotope fractionation. During hydrolysis at pH 9, the S_N2-type displacement reaction cleaving the C-O bond affects the carbon isotope fractionation and contributes to 67 - 80% of the overall reaction. The radical oxidation of TBP results in $AKIE_C$ and $AKIE_H$ of 1.007 – 1.011 and 1.608 - 2.174, respectively, which is consistent with a major contribution of a C-H bond cleavage. The correlation of ^2H and ^{13}C isotope fractionation of TBP allows identifying radical reactions and distinguishing radical reactions from hydrolysis.

Acknowledgements

Jia Liu and Langping Wu were financially supported by the China Scholarship Council (File No. 201506460057 and 201306460007, respectively). The work was partially supported by the National Science Foundation of China [grant number 41430106, 2014 and 41573080, 2015]. The authors are grateful for using the analytical facilities of the Centre for Chemical Microscopy (ProVIS) at the Helmholtz Centre for Environmental Research – UFZ, which is supported by the European Regional Development Funds (EFRE - Europe funds Saxony) and the Helmholtz Association. The authors thank Dr. Oliver J. Lechtenfeld for his support on transformation products analysis in ProVIS, and thank Dr. Matthias Gehre for his help in the Isotope Laboratory of the UFZ. We are grateful to Axel Horst for critical reading of our manuscript.

Conflicts of interest: none.

References

Bacaloni, A., Cucci, F., Guarino, C., Nazzari, M., Samperi, R., Laganà, A., 2008. Occurrence of organophosphorus flame retardant and plasticizers in three volcanic lakes of central Italy. Environ. Sci. Technol. 42, 1898-1903.

Bergman, A., Ryden, A., Law, R.J., de Boer, J., Covaci, A., Alaee, M., Birnbaum, L., Petreas, M., Rose, M., Sakai, S., Van den Eede, N., van der Veen, I., 2012. A novel abbreviation standard for organobromine, organochlorine and organophosphorus flame retardants and some characteristics of the chemicals. Environ. Int. 49, 57-82.

Berne, C., Allainmat, B., Garcia, D., 2005. Tributyl phosphate degradation by Rhodopseudomonas palustris and other photosynthetic bacteria. Biotechnol. Lett. 27, 561-566.

Blumenthal, E., Herbert, J., 1945. The mechanism of the hydrolysis of trimethyl orthophosphate. Trans. Faraday Soc. 41, 611-617.

Bouchard, D., Hunkeler, D., Höhener, P., 2008. Carbon isotope fractionation during aerobic biodegradation of n-alkanes and aromatic compounds in unsaturated sand. Org. Geochem. 39, 23-33.

Buxton, G.V., Greenstock, C.L., Helman, W.P., Ross, A.B., 1988. Critical review of rate constants for reactions of hydrated electrons, hydrogen atoms and hydroxyl radicals (·OH/·O−) in aqueous solution. J. Phys. Chem. Ref. Data 17, 513-886.

Coplen, T.B., 1996. New guidelines for reporting stable hydrogen, carbon, and oxygen isotope-ratio data. Geochim. Cosmochim. Acta 60, 3359-3360.

Day, J.N.E., Ingold, C.K., 1941. Mechanism and kinetics of carboxylic ester hydrolysis and carboxyl esterification. Trans. Faraday Soc. 1941, 686-705.

Elsner, M., 2010. Stable isotope fractionation to investigate natural transformation mechanisms of organic contaminants: principles, prospects and limitations. J. Environ. Monit. 12, 2005-2031.

Elsner, M., Zwank, L., Hunkeler, D., Schwarzenbach, R.P., 2005. A new concept linking observable stable isotope fractionation to transformation pathways of organic pollutants. Environ. Sci. Technol. 39, 6896-6916.

Fries, E., Püttmann, W., 2003. Monitoring of the three organophosphate esters TBP, TCEP and TBEP in river water and ground water (Oder, Germany). J. Environ. Monit. 5, 346-352.

Gray, J.R., Lacrampe-Couloume, G., Gandhi, D., Scow, K.M., Wilson, R.D., Mackay, D.M., Sherwood Lollar, B., 2002. Carbon and hydrogen isotopic fractionation during biodegradation of methyl tert-butyl ether. Environ. Sci. Technol. 36, 1931-1938.

Greget, R., Dadak, S., Barbier, L., Lauga, F., Linossier-Pierre, S., Pernot, F., Legendre, A., Ambert, N., Bouteiller, J.M., Dorandeu, F., Bischoff, S., Baudry, M., Fagni, L., Moussaoui, S., 2016. Modeling and simulation of organophosphate-induced neurotoxicity: Prediction and validation by experimental studies. Neurotoxicology 54, 140-152.

He, X., Mezyk, S.P., Michael, I., Fatta-Kassinos, D., Dionysiou, D.D., 2014. Degradation kinetics and mechanism of beta-lactam antibiotics by the activation of H2O2 and Na2S2O8 under UV-254nm irradiation. J. Hazard. Mater. 279, 375-383.

Herrmann, H., 2003. Kinetics of aqueous phase reactions relevant for atmospheric chemistry. Chem. Rev. 103, 4691-4716.

Herrmann, H., 2007. On the photolysis of simple anions and neutral molecules as sources of O-/OH, SOx- and Cl in aqueous solution. Phys. Chem. Chem. Phys. 9, 3935-3964.

Herrmann, H., Reese, A., Zellner, R., 1995. Time-resolved UV/VIS diode array absorption spectroscopy of SOx−(x=3, 4, 5) radical anions in aqueous solution. J. Mol. Struct. 348, 183-186.

House, D.A., 1962. Kinetics and Mechanism of Oxidations by Peroxydisulfate. Chem. Rev. 62, 185-&.

Kirby, A.J., Mora, J.R., Nome, F., 2013. New light on phosphate transfer from triesters. Biochim. Biophys. Acta. 1834, 454-463.

Lau, T.K., Chu, W., Graham, N.J., 2007. The aqueous degradation of butylated hydroxyanisole by UV/S2O82-: study of reaction mechanisms via dimerization and mineralization. Environ. Sci. Technol. 41, 613-619.

Lee, S., Jeong, W., Kannan, K., Moon, H.B., 2016. Occurrence and exposure assessment of organophosphate flame retardants (OPFRs) through the consumption of drinking water in Korea. Water Res. 103, 182-188.

Liang, C., Su, H.-W., 2009. Identification of sulfate and hydroxyl radicals in thermally activated persulfate. Ind. Eng. Chem. Res. 48, 5558-5562.

Martinez-Carballo, E., Gonzalez-Barreiro, C., Sitka, A., Scharf, S., Gans, O., 2007. Determination of selected organophosphate esters in the aquatic environment of Austria. Sci. Total Environ. 388, 290-299.

Mincher, B.J., Mezyk, S.P., Martin, L.R., 2008. A pulse radiolysis investigation of the reactions of tributyl phosphate with the radical products of aqueous nitric acid irradiation. J. Phys. Chem. A 112, 6275-6280.

Nancharaiah, Y.V., Reddy, G.K.K., Mohan, T.V.K., Venugopalan, V.P., 2015. Biodegradation of tributyl phosphate, an organosphate triester, by aerobic granular biofilms. J. Hazard. Mater. 283, 705-711.

Neta, P., Huie, R.E., Ross, A.B., 1988. Rate constants for reactions of inorganic radicals in aqueous solution. J. Phys. Chem. Ref. Data 17, 1027-1284.

Nijenhuis, I., Richnow, H.H., 2016. Stable isotope fractionation concepts for characterizing biotransformation of organohalides. Curr. Opin. Biotechnol. 41, 108-113.

Northrop, D.B., 1981. The expression of isotope effects on enzyme-catalyzed reactions. Annual review of biochemistry 50, 103-131.

Oh, Y.-C., Bao, Y., Jenks, W.S., 2003. Isotope studies of photocatalysis: TiO2-mediated degradation of dimethyl phenylphosphonate. J. Photoch. Photobio. A: Chem 161, 69-77.

Ou, H.s., Liu, J., Ye, J.s., Wang, L.l., Gao, N.y., Ke, J., 2017. Degradation of tris(2-chloroethyl) phosphate by ultraviolet-persulfate: Kinetics, pathway and intermediate impact on proteome of Escherichia coli. Chem. Eng. J. 308, 386-395.

Paneth, P., Buncel, E., Saunders Jr, W., 1992. Isotopes in Organic Chemistry Vol. 8. Elsevier, New York.

Rayleigh, L., 1896. L.Theoretical considerations respecting the separation of gases by diffusion and similar processes. Philos. Mag. 42, 493-498.

Regnery, J., Puttmann, W., 2010. Occurrence and fate of organophosphorus flame retardants and plasticizers in urban and remote surface waters in Germany. Water Res.

44, 4097-4104.

Regnery, J., Puttmann, W., Merz, C., Berthold, G., 2011. Occurrence and distribution of organophosphorus flame retardants and plasticizers in anthropogenically affected groundwater. J. Environ. Monit. 13, 347-354.

Rodil, R., Quintana, J.B., Concha-Grana, E., Lopez-Mahia, P., Muniategui-Lorenzo, S., Prada-Rodriguez, D., 2012. Emerging pollutants in sewage, surface and drinking water in Galicia (NW Spain). Chemosphere 86, 1040-1049.

Russell, G.A., 1957. Deuterium-isotope effects in the autoxidation of aralkyl hydrocarbons. Mechanism of the interaction of peroxy radicals. J. Am. Chem. Soc. 79, 3871-3877.

Shi, Y., Gao, L., Li, W., Wang, Y., Liu, J., Cai, Y., 2016. Occurrence, distribution and seasonal variation of organophosphate flame retardants and plasticizers in urban surface water in Beijing, China. Environ. Pollut. 209, 1-10.

Su, G., Letcher, R.J., Yu, H., 2016. Organophosphate Flame Retardants and Plasticizers in Aqueous Solution: pH-Dependent Hydrolysis, Kinetics, and Pathways. Environ. Sci. Technol. 50, 8103-8111.

Thullner, M., Centler, F., Richnow, H.-H., Fischer, A., 2012. Quantification of organic pollutant degradation in contaminated aquifers using compound specific stable isotope analysis – Review of recent developments. Org. Geochem. 42, 1440-1460.

Van Breukelen, B.M., 2007. Extending the Rayleigh equation to allow competing isotope fractionating pathways to improve quantification of biodegradation. Environ. Sci. Technol. 41, 4004-4010.

Vogt, C., Dorer, C., Musat, F., Richnow, H.H., 2016. Multi-element isotope fractionation concepts to characterize the biodegradation of hydrocarbons - from enzymes to the environment. Curr. Opin. Biotechnol. 41, 90-98.

Waclawek, S., Lutze, H.V., Grubel, K., Padil, V.V.T., Cernik, M., Dionysiou, D.D., 2017. Chemistry of persulfates in water and wastewater treatment: A review. Chem. Eng. J. 330, 44-62.

Wanamaker, E.C., Chingas, G.C., McDougal, O.M., 2013. Parathion hydrolysis revisited: in situ aqueous kinetics by 1H NMR. Environ. Sci. Technol. 47, 9267-9273.

Watts, M.J., Linden, K.G., 2009. Advanced oxidation kinetics of aqueous tri alkyl phosphate flame retardants and plasticizers. Environ. Sci. Technol. 8, 2937-2942.

Watts, R.J., Teel, A.L., 2006. Treatment of contaminated soils and groundwater using ISCO. Practice Periodical of Hazardous, Toxic, and Radioactive Waste Management 10, 2-9.

Wolfsberg, M., Van Hook, W.A., Paneth, P., Rebelo, L.P.N., 2009. Isotope effects: in the chemical, geological, and bio sciences. Springer Science & Business Media.

Wu, L., Chládková, B., Lechtenfeld, O.J., Lian, S., Schindelka, J., Herrmann, H., Richnow, H.H., 2018a. Characterizing chemical transformation of organophosphorus compounds by 13C and 2H stable isotope analysis. Sci. Total Environ. 615, 20-28.

Wu, L., Kummel, S., Richnow, H.H., 2017. Validation of GC-IRMS techniques for δ13C and δ2H CSIA of organophosphorus compounds and their potential for studying the mode of hydrolysis in the environment. Anal. Bioanal. Chem. 409, 2581-2590.

Wu, L., Verma, D., Bondgaard, M., Melvej, A., Vogt, C., Subudhi, S., Richnow, H.H., 2018b. Carbon and hydrogen isotope analysis of parathion for characterizing its natural attenuation by hydrolysis at a contaminated site. Water Res. 143, 146-154.

Wu, L., Yao, J., Trebse, P., Zhang, N., Richnow, H.H., 2014. Compound specific isotope analysis of organophosphorus pesticides. Chemosphere 111, 458-463.

Wu, T., Gan, Q., Jans, U., 2006. Nucleophilic substitution of phosphorothionate ester pesticides with bisulfide (HS-) and polysulfides (Sn2-). Environ. Sci. Technol. 40, 5428-5434.

Yang, Y., Lu, X., Jiang, J., Ma, J., Liu, G., Cao, Y., Liu, W., Li, J., Pang, S., Kong, X., Luo, C., 2017. Degradation of sulfamethoxazole by UV, UV/H2O2 and UV/persulfate (PDS): Formation of oxidation products and effect of bicarbonate. Water Res. 118, 196-207.

Zhang, N., Geronimo, I., Paneth, P., Schindelka, J., Schaefer, T., Herrmann, H., Vogt, C., Richnow, H.H., 2016. Analyzing sites of OH radical attack (ring vs. side chain) in oxidation of substituted benzenes via dual stable isotope analysis (δ13C and δ2H). Sci. Total Environ. 542, 484-494.

Table 1. Pseudo-first order kinetic rate constants (k_{obs}), isotope enrichment factors (ε), AKIE and Λ values obtained from the hydrolysis and the radical oxidation of TBP at different pH.

Conditions	k_{obs} ($\times 10^{-3} h^{-1}$)	Temp. ^{0}C	TBP:oxidant molar ratio	Major radicals	$\Delta\delta^{13}C$[h] (‰)	$\Delta\delta^{2}H$[h] (‰)	ε_C(‰)	R^2_C	ε_H(‰)	R^2_H	$AKIE_C$	$AKIE_H$	Λ	R^2_Λ
Hydrolysis														
pH 2	2.0±0.3 [a]	80			9.1		-3.8±0.3	0.990	n.d.[b]		1.048±0.004	n.c.[c]	n.d.	
pH 7	1.8±0.2	80			9.9		-4.6±0.5	0.990	n.d.		1.058±0.007	n.c.	n.d.	
pH 9	4.0±0.5	80			8.3		-2.8±0.1	0.997	n.d.		n.c.	n.c.	n.d.	
pH 12	1.1±0.2	35					n.d.		n.d.		n.c.	n.c.	n.d.	
Radical oxidation														
pH7/KPS	10.4±0.4	35	1:20	SO_4•-	2.7	52	-0.9±0.1	0.986	-16±2	0.987	1.011±0.001	1.761±0.167	17±1	0.996
pH9/KPS	8.8±1.1	35	1:20	SO_4•-,•OH	2.1	51	-0.8±0.1	0.989	-20±2	0.991	1.010±0.001	2.174±0.255	23±1	0.990
pH12/KPS	5.5±0.3	35	1:20	•OH	1.1	21	-0.5±0.1	0.980	-11±1	0.993	n.c.	n.c.	19±1	0.991
[d]pH7/UV/H_2O_2_1	474.2±11.4	20	1:5	•OH	2.4	38	-0.8±0.1	0.995	-14±1	0.993	1.010±0.001	1.608±0.070	17±1	0.996
[e]pH7/UV/H_2O_2_2	27.9±2.4	15	1:5	•OH	1.3	23	-0.6±0.3	0.928	-13±3	0.985	1.007±0.004	1.610±0.209	19±7	0.956
[e]pH7/UV/H_2O_2_3	6.8±0.5	15	1:5	•OH	1.6	40	-0.6±0.2	0.972	-17±7	0.983	1.007±0.001	1.761±0.418	25±6	0.994
[f]pH7/UV/H_2O_2_ave.							-0.7±0.1[e]		-15±2[e]				20±4[e]	
[g]average							-0.7±0.1[f]		-16±3[f]				20±4[f]	

a: "±" indicates the 95% confidence interval; b: "n.d." is short for not detected; c: "n.c." is short for not calculated;

d-e: the distance between the photo-reactor and light source was 13 cm and 22 cm, respectively;

f: average values of ε and Λ for UV/H_2O_2 experiment, calculating from the three individual UV/H_2O_2 experiments;

g: average values of ε and Λ for radical oxidation of TBP, calculating from all individual radical oxidation experiments expect pH 12/KPS.

h: isotope shifts of the $\delta^{13}C$ and $\delta^{2}H$ values from the first and last sampling points during the degradation period.

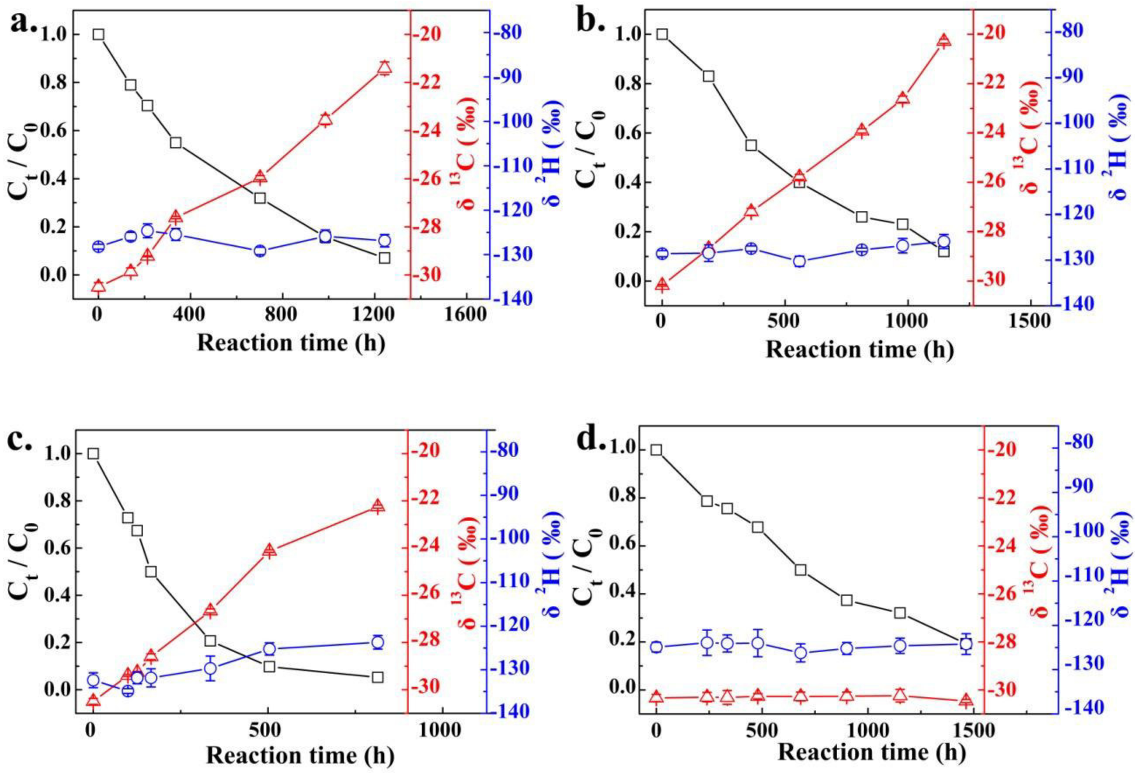

Fig. 1: TBP degradation via hydrolysis at (a) pH 2, (b) pH 7, (c) pH9, and (d) pH 12. Changes in concentrations (C_t/C_0, black squares) are correlated with the changes of the carbon ($\delta^{13}C$, red triangles) and hydrogen isotope ratios ($\delta^{2}H$, blue circles).

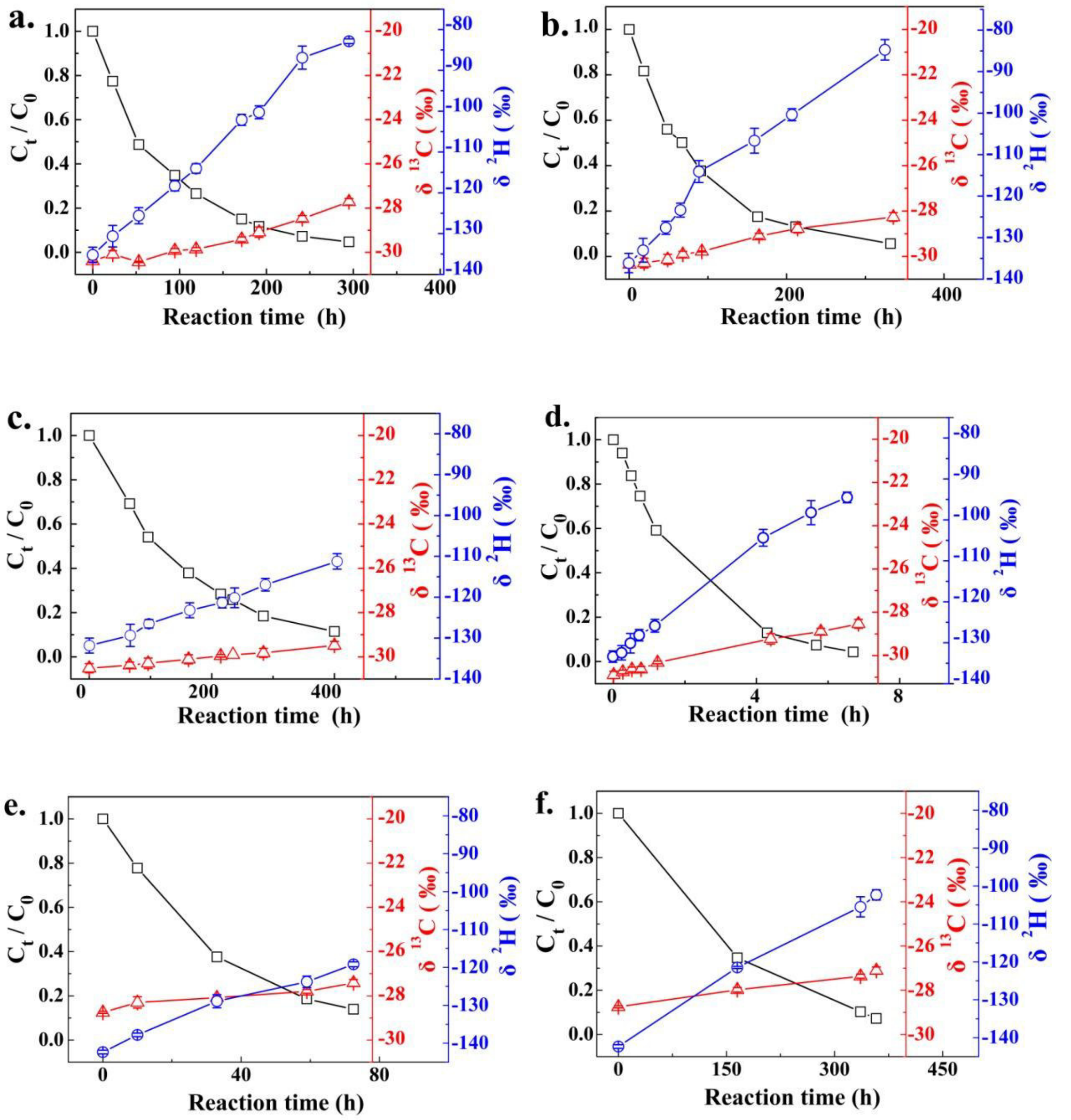

Fig. 2: TBP degradation via radical oxidation. Reaction conditions were as follows: (a) pH7/KPS; (b) pH9/KPS; (c) pH12/KPS; (d) UV/H_2O_2_1; (e) UV/H_2O_2_2; (f) UV/H_2O_2_3. Changes in concentrations (C_t/C_0, black squares) are correlated with changes of the carbon ($\delta^{13}C$, red triangles) and hydrogen isotope ratios (δ^2H, blue circles).

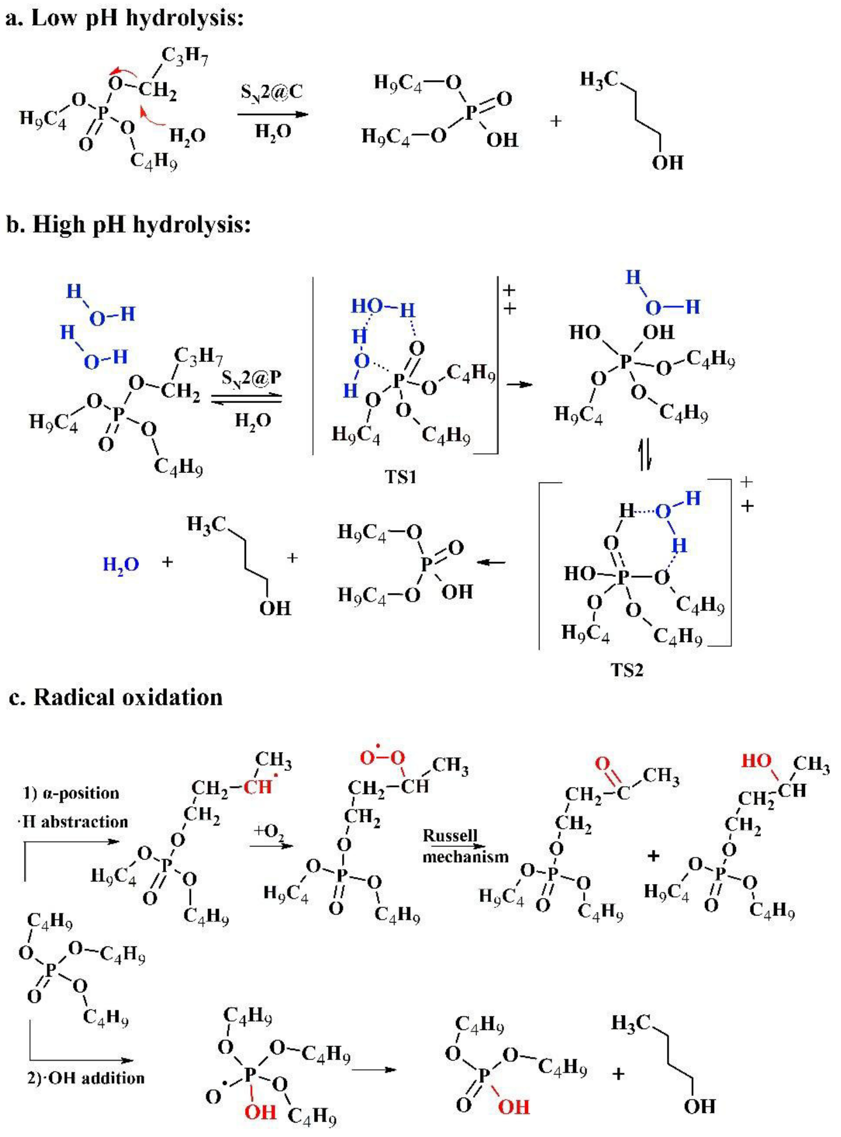

Fig. 3: Proposed transformation mechanisms of TBP via hydrolysis and radical oxidation. Hydrolysis of TBP occurs via two pathways: (a) attacked by H_2O at the α-carbon with S_N2-type substitution at low pH or (b) attacked by H_2O at the P atom with S_N2-type substitution at high pH. The latter reaction is accompanied with two transition states. Three water molecules assisting the hydrolysis reaction by allowing two proton transfers, via a concerted six-membered cyclic activated complex (TS1) that includes general base catalysis in the first step and the cleavage of the pentacoordinated intermediate in the second step (TS2). The radical oxidation by $^{\bullet}OH$ can process via two mechanisms. Both processes can occur simultaneously: (1). H-abstraction by $^{\bullet}OH$, followed by an oxygen addition and finally undergoing the Russell mechanism; (2). the $^{\bullet}OH$ addition formed the $(ButO)_2POC{\cdot}HC_3H_7$ radical followed by the elimination of butanol.

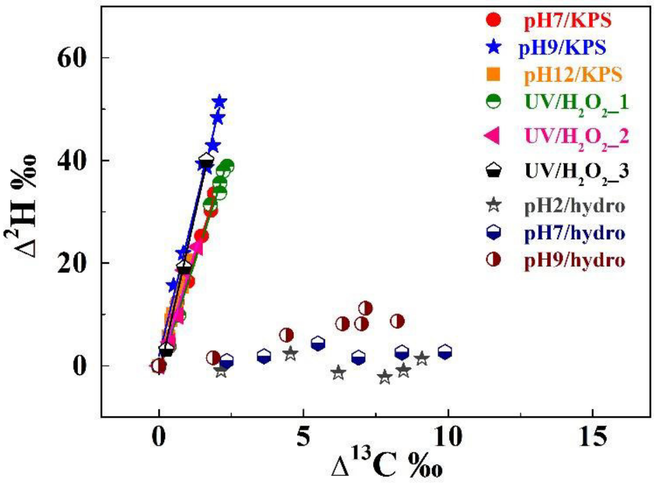

Fig. 4: Two dimensional isotope plots for TBP degradation via hydrolysis and radical oxidation.

Figure captions

Fig. 1. TBP degradation via hydrolysis at different pH. Changes in concentrations (C_t/C_0) are correlated to changes in the carbon ($\delta^{13}C$) and hydrogen isotope ratios (δ^2H).

Fig. 2. TBP degradation via radical oxidation. Changes in concentrations (C_t/C_0) are correlated with changes in the carbon ($\delta^{13}C$) and hydrogen isotope ratios (δ^2H).

Fig. 3. Proposed transformation mechanisms of TBP via hydrolysis and radical oxidation.

Fig. 4. Two dimensional isotope plots for TBP degradation via hydrolysis and radical oxidation.

Supplementary Material 2